

The Energy Balance of the Earth's Surface

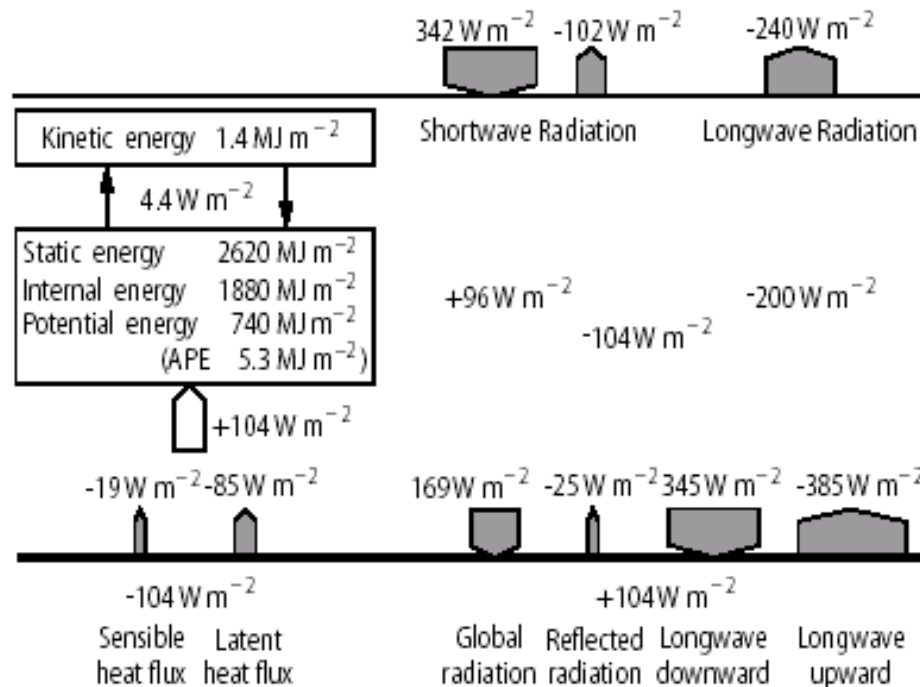


Fig. 10.5 Redistribution of radiative energy in the climate system (from 98Wil and 04Ohm). All values refer to a mean solar constant of 1368 W m^{-2} and are global annual averages. Note the large amount of surplus heat at the surface, which must be removed from the surface by turbulent fluxes of latent and sensible heat. The radiation budget of the atmosphere alone is negative, requiring an amount of about 104 W m^{-2} to be added from ground by evapotranspiration and fluxes of sensible heat.

Ohmura and Raschke (2005)

The energy exchange between the earth's surface and the atmosphere is one of the driving mechanisms of the climate system. According to Ohmura and Raschke (2005), 60% of the total absorption of solar radiation by the atmosphere/earth's surface system takes place at the surface.

Definition of the surface energy balance

The surface energy balance is usually defined with respect to an active layer of infinitesimal small thickness. In this case the storage of energy in the layer can be neglected and the energy balance equation takes the form:

$$S(1 - \alpha) + L\downarrow - L\uparrow + H + L_v E + G = 0$$

or, summarizing the radiation fluxes:

$$NR + H + L_v E + G = 0$$

where

NR = net radiation

S = global solar radiation (direct plus diffuse radiation)

α = albedo

$L\downarrow$ = incoming (atmospheric) longwave radiation

$L\uparrow$ = outgoing (terrestrial) longwave radiation

H = sensible heat flux

$L_v E$ = latent heat flux of vaporisation

G = ground heat flux

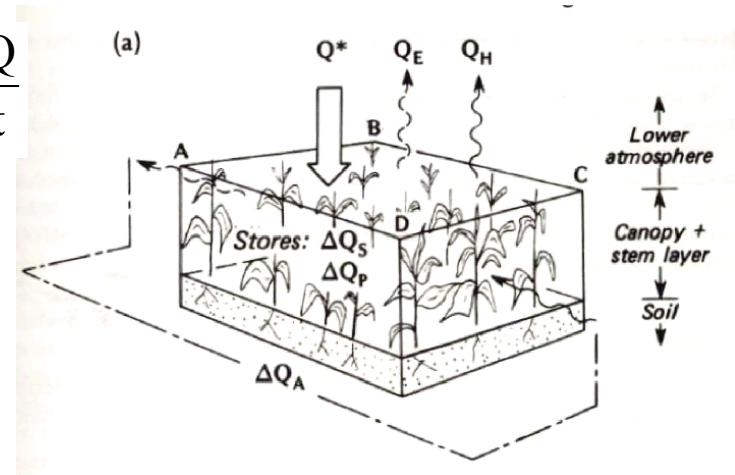
Fluxes are considered positive when directed toward the surface (energy sources) and negative when directed away from the surface (energy sinks). Exceptions are $L\uparrow$ and αS (outgoing radiation fluxes), for which a minus sign is explicitly used in the energy balance equation.

The energy balance of a volume

In other situations, however, the active layer has a measurable thickness. In this case the rate of change of energy stored in the layer, $\partial Q/\partial t$, must be included in the equation:

$$NR + H + L_v E + G = \frac{\partial Q}{\partial t}$$

In many instances we also need to take the lateral fluxes (advection) into account.



Oke (1987)

This situation is encountered for instance with vegetation or snow. In the latter case, part of the heat supplied to or removed from the snow volume may eventually lead to melt ($M > 0$) or freezing ($M < 0$), and:

$$NR + H + L_v E + G = \frac{\partial Q}{\partial t} + L_f M$$

where $L_f = 0.334 \cdot 10^6 \text{ J kg}^{-1}$ is the latent heat of fusion.



A spatial look at the surface energy balance

The first attempt to produce an atlas of the surface energy balance is due to Budyko (1956) and the results are summarized in Budyko (1974).

The results presented here are taken from Raschke and Ohmura (2005) and Ohmura and Raschke (2005). They are based on satellite measurements from the International Satellite Clouds Climatology Project (ISCCP) and data from the Reanalysis Project of the European Centre for Medium-Range Weather Forecasts (ECMWF ReAnalysis, ERA-40).

References

Budyko, M.I., 1974, *Climate and Life. International Geophysical Series, Vol. 18*. Academic Press, New York, 508 pp.

Ohmura, A. and E. Raschke, 2005, *Energy Budget at the Earth's Surface*. In: Hantel., M. (Ed.), *Observed Global Climate, Landold-Börnstein, V/6 (Geophysics/Climatology)*, Springer.

Raschke, E. and A. Ohmura, 2005, *Radiation Budget of the Climate System*. In: Hantel., M. (Ed.), *Observed Global Climate, Landold-Börnstein, V/6 (Geophysics/Climatology)*, Springer.

A spatial look at the surface energy balance (2)

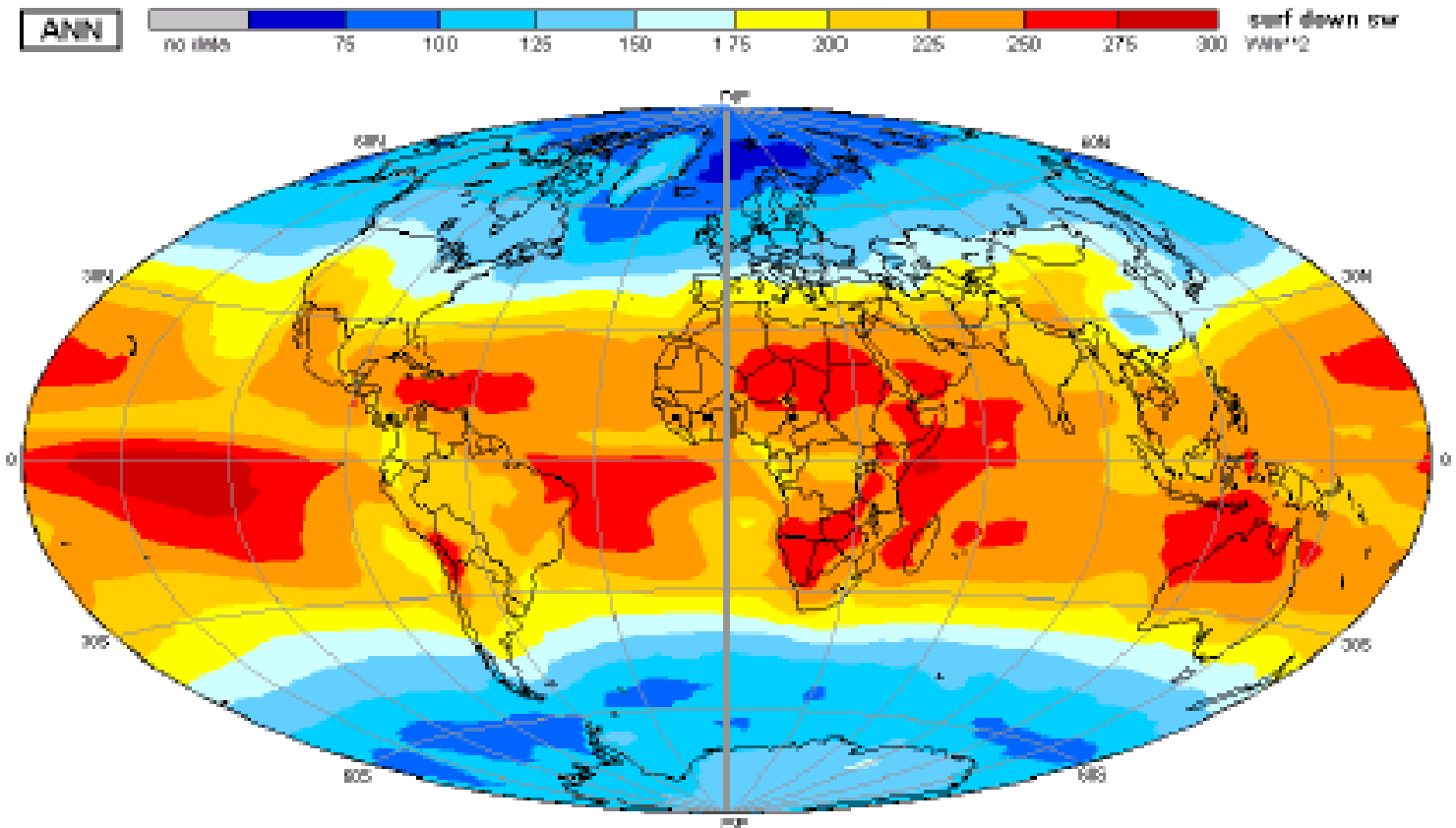


Fig. 4.3.4.3a Annual average of the downward solar radiation at ground during the period 1991 to 1995 in Wm^{-2} . Prime modifiers of these fields are the mean solar height over each area and the persistence and thickness of cloud fields. Note the low amounts over southern China. Extreme small values are obtained over the northernmost Atlantic Ocean. Highest and lowest values: 286 and 60 Wm^{-2} ; global average: 189 Wm^{-2} . The values are possibly too high by about 5 to 10 Wm^{-2} as preliminary comparisons with ground-based measurements have shown.

A spatial look at the surface energy balance (3)

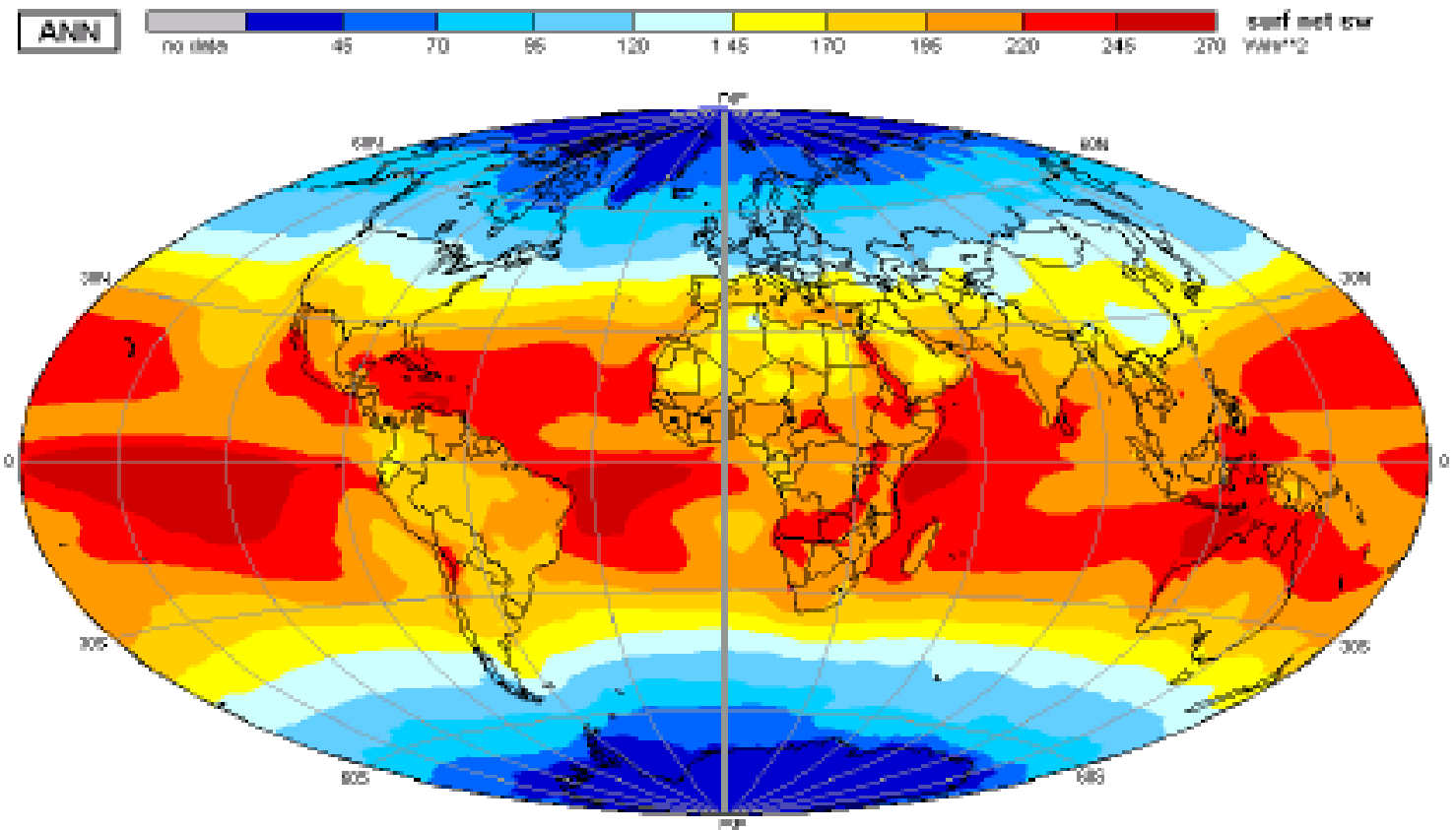


Fig. 4.3.4.4 Annual average of the solar net radiation at ground, which is the downward solar minus reflected fraction of it during the period 1991 to 1995, in Wm^{-2} . This map identifies the regions with low surface albedo and low cloudiness to gain highest amounts of incoming radiation. Highest and lowest values: 270 and 22 Wm^{-2} ; global average: 165 Wm^{-2} .

A spatial look at the surface energy balance (4)

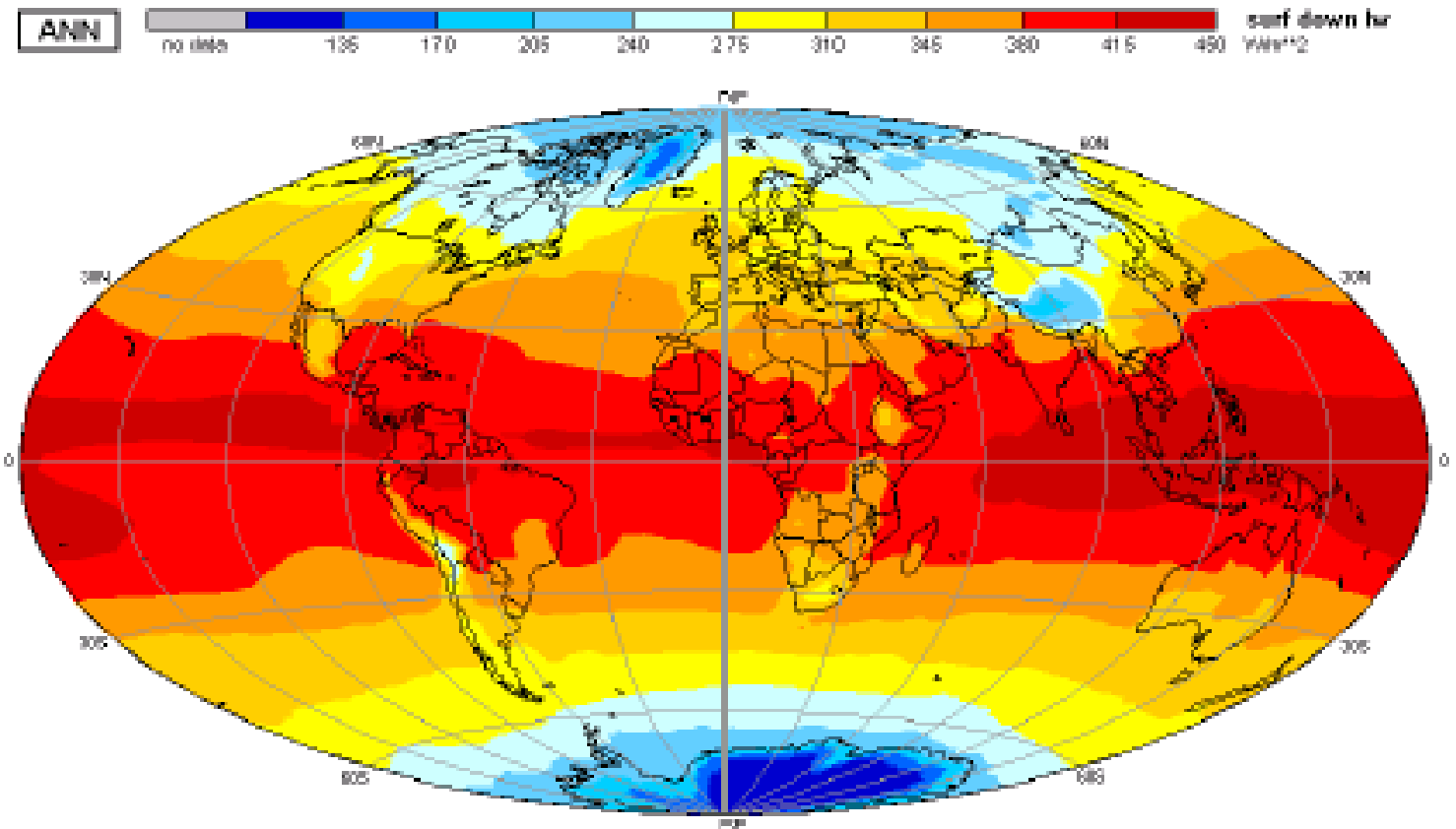


Fig. 4.3.4.5 Annual average of the downward terrestrial (atmospheric) radiation at ground during the period 1991 to 1995, in Wm^{-2} . These fields are dominated by the temperature and water vapor content of the lower troposphere and at higher latitudes also by cloud base heights. Highest and lowest values: 431 and 101 Wm^{-2} ; global average: 343 Wm^{-2} .

A spatial look at the surface energy balance (5)

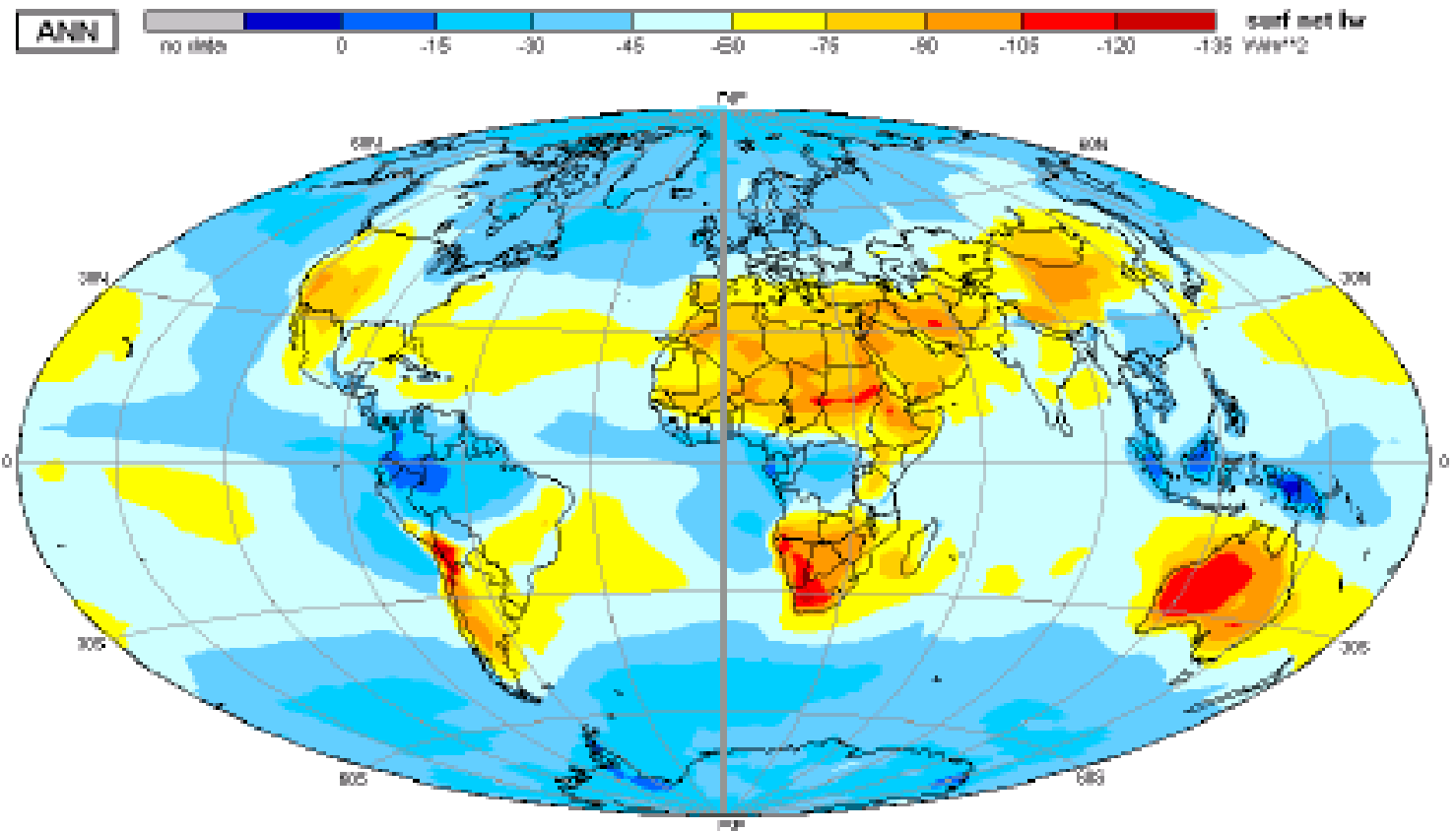


Fig. 4.3.4.6 Annual average of the net fluxes of terrestrial radiation at ground, computed from the difference between the downward atmospheric and the upward surface heat radiation during the period 1991 to 1995, in Wm^{-2} . All values are negative indicating, that in the average the ground heats the atmosphere above. Highest and lowest values are -10 and -134 Wm^{-2} , global average : -50 Wm^{-2} .

A spatial look at the surface energy balance (6)

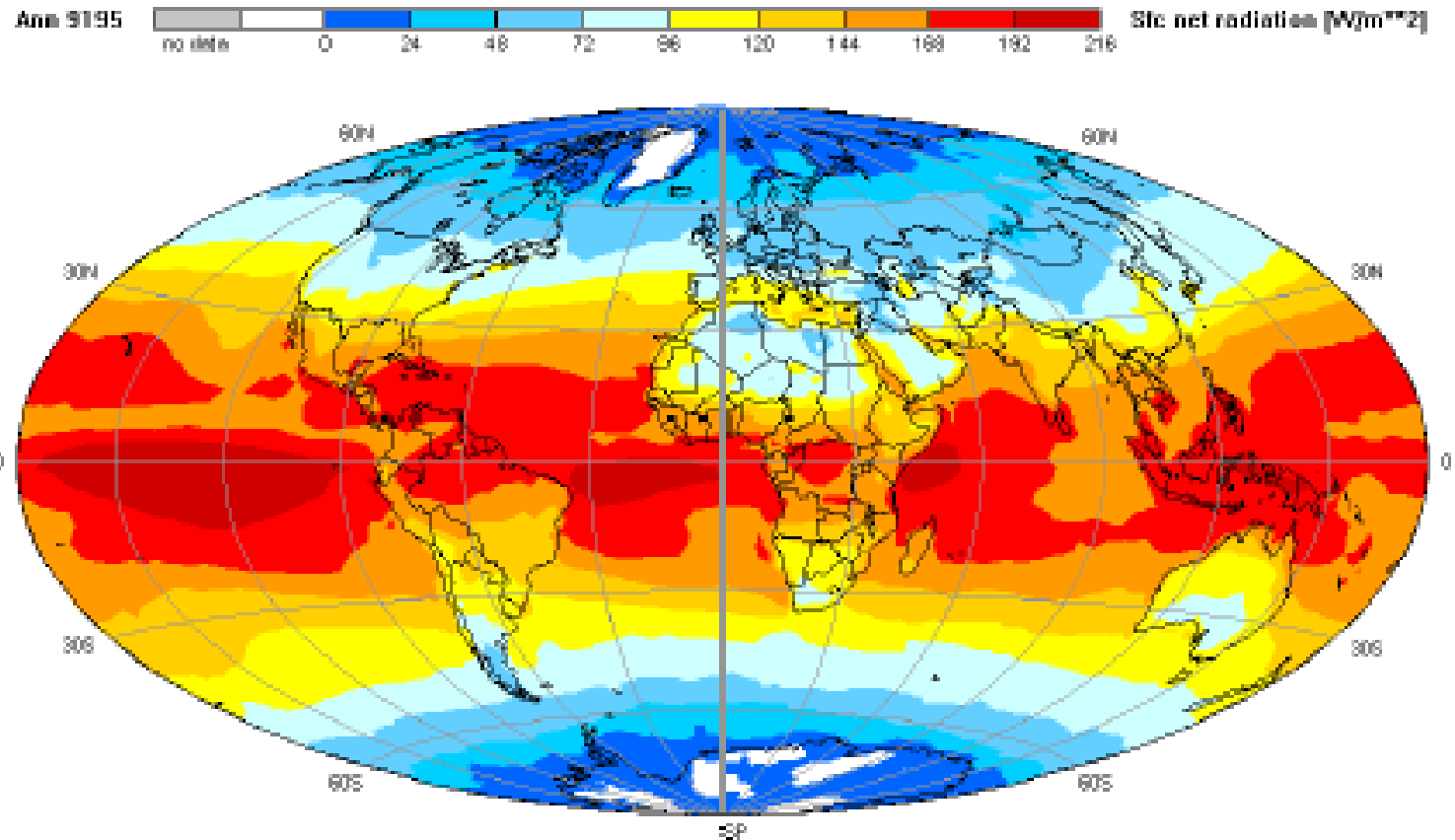


Fig. 4.3.4.7 Annual average of the total net radiation (or of the radiation budget) at the surface during the period 1991 to 1995, in Wm^{-2} . All values, with a few exceptions over Greenland and Antarctica, are positive indicating, that the Earth's surface is everywhere heated by radiation. The small negative white areas are very close to zero. They are possibly caused by errors in both components over those regions, due to inaccurate cloud identification over those regions. Highest and lowest values: $+211$ and -16 Wm^{-2} ; global average: $+116 \text{ Wm}^{-2}$.

A spatial look at the surface energy balance (7)

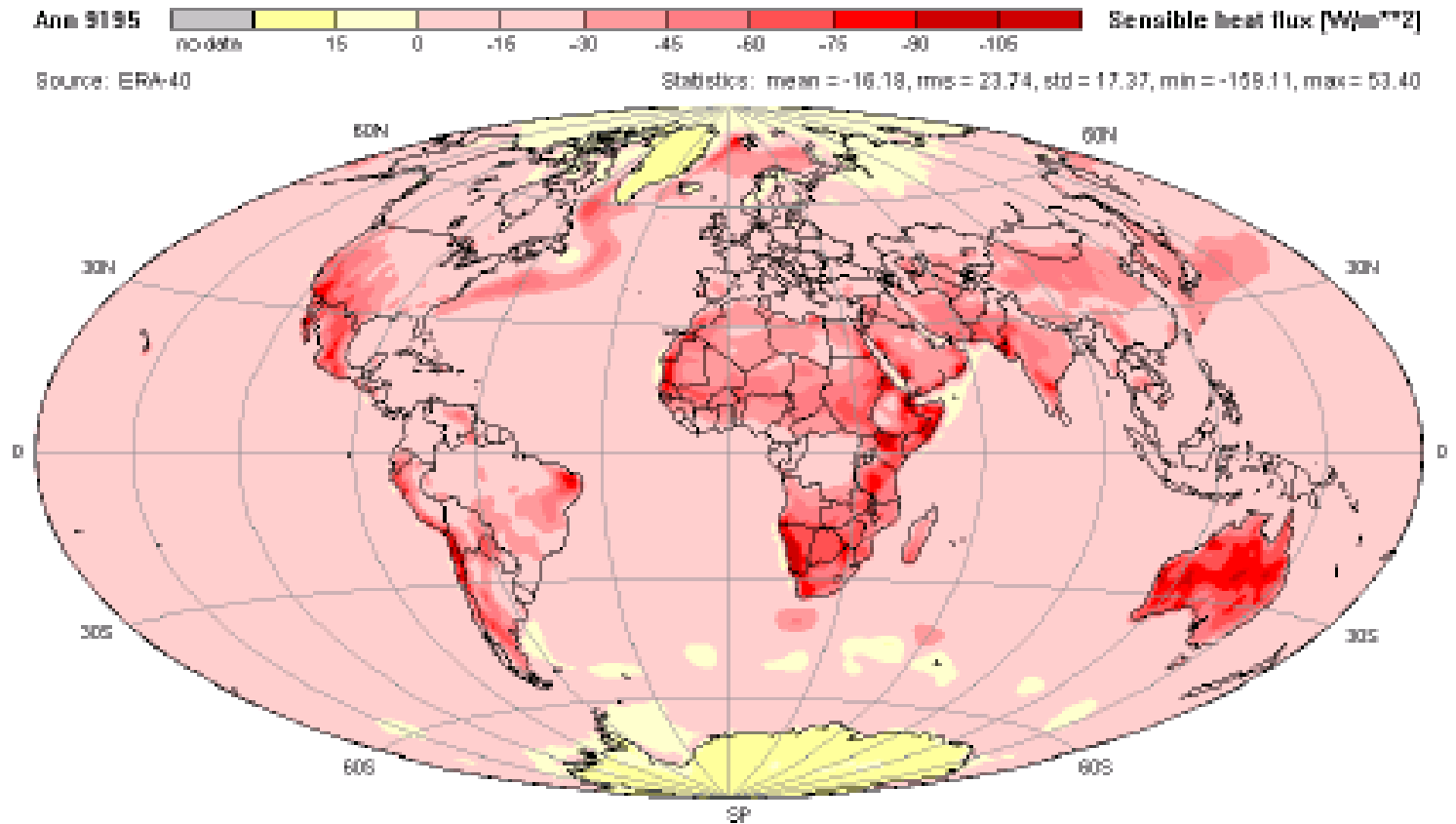


Fig. 10.3a Annual mean distribution of sensible heat fluxes, based on data of the re-analysis project ERA-40. This data set covers the period 1991-1995. Note the downward fluxes of sensible heat over larger ice fields and some sections of the Southern Oceans.

A spatial look at the surface energy balance (8)

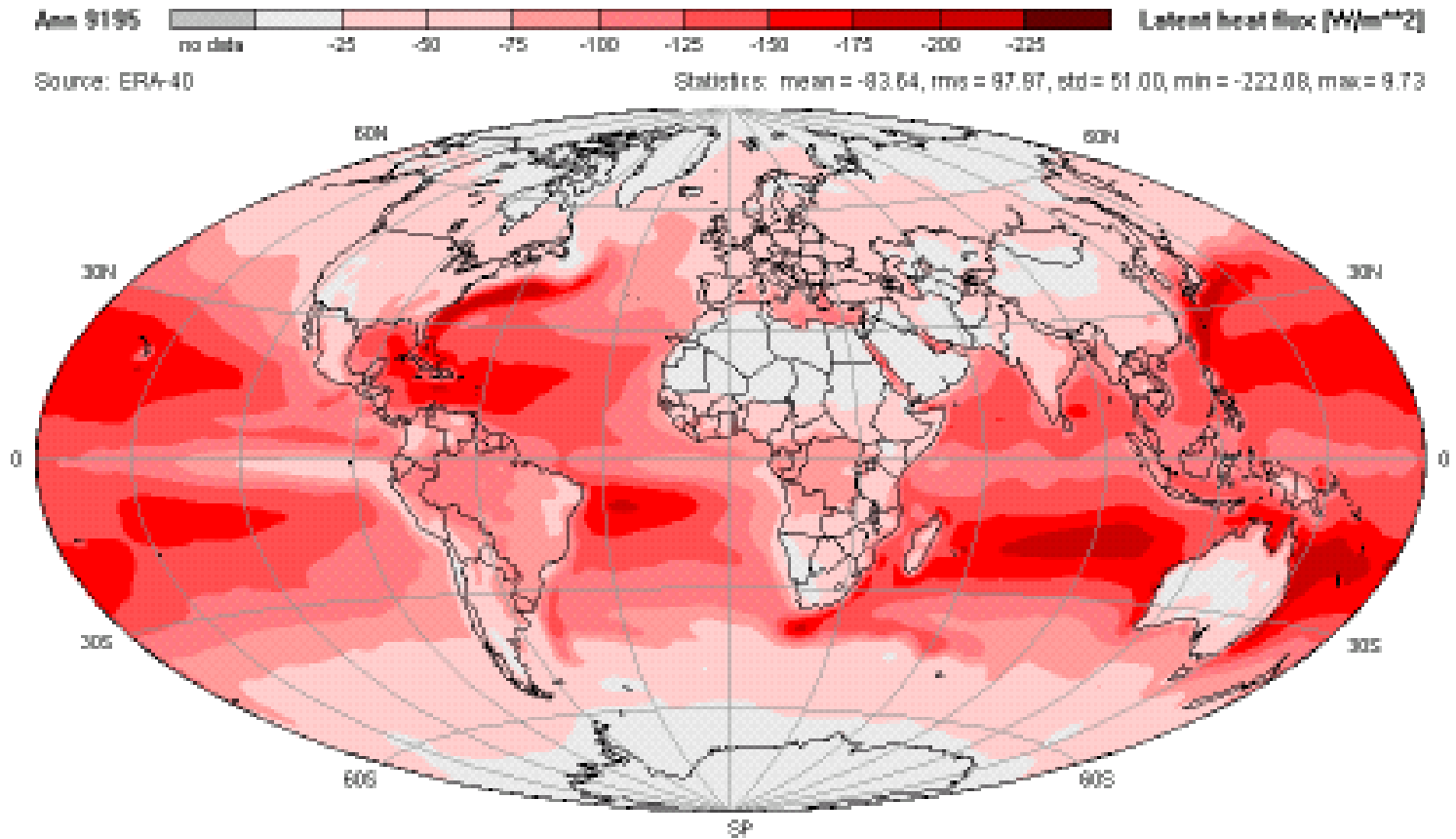
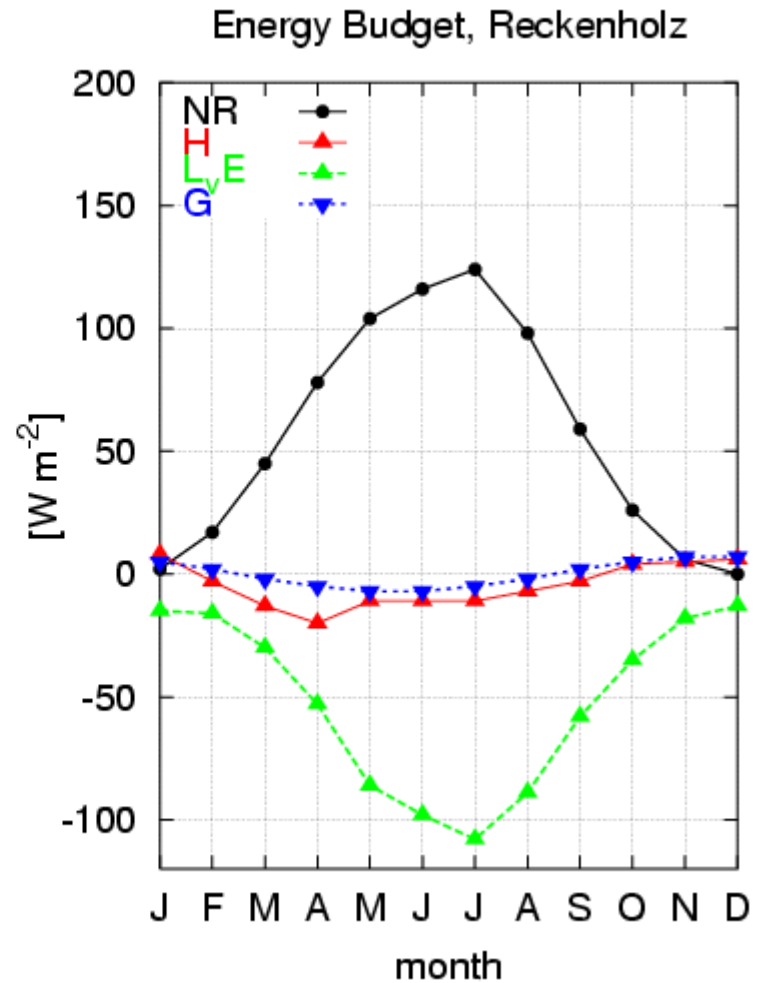
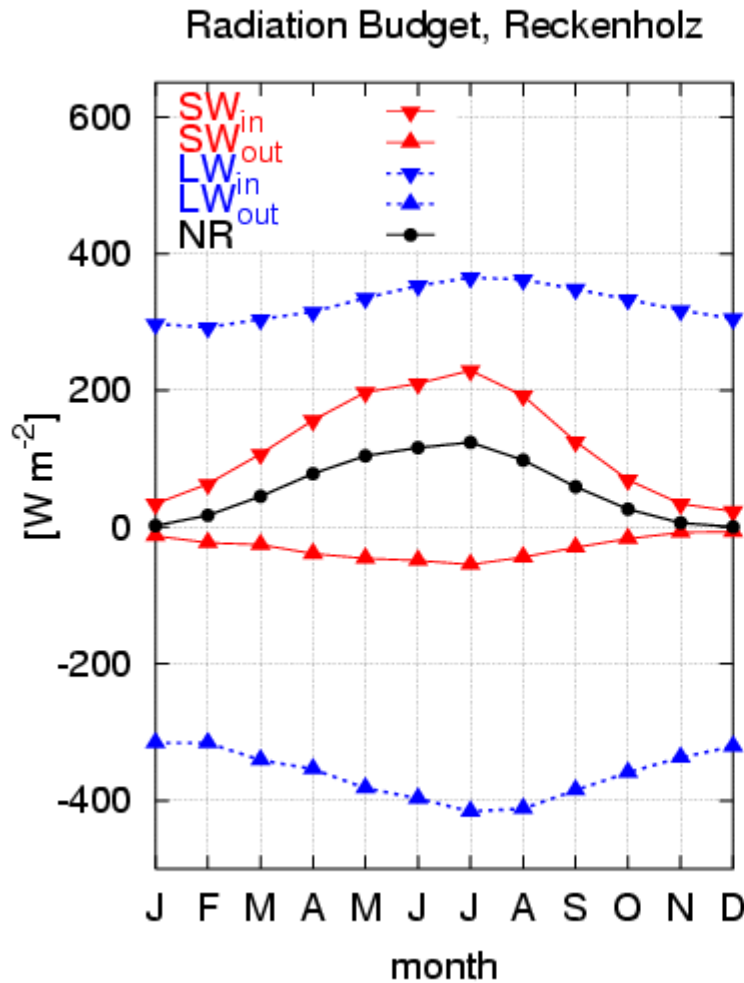


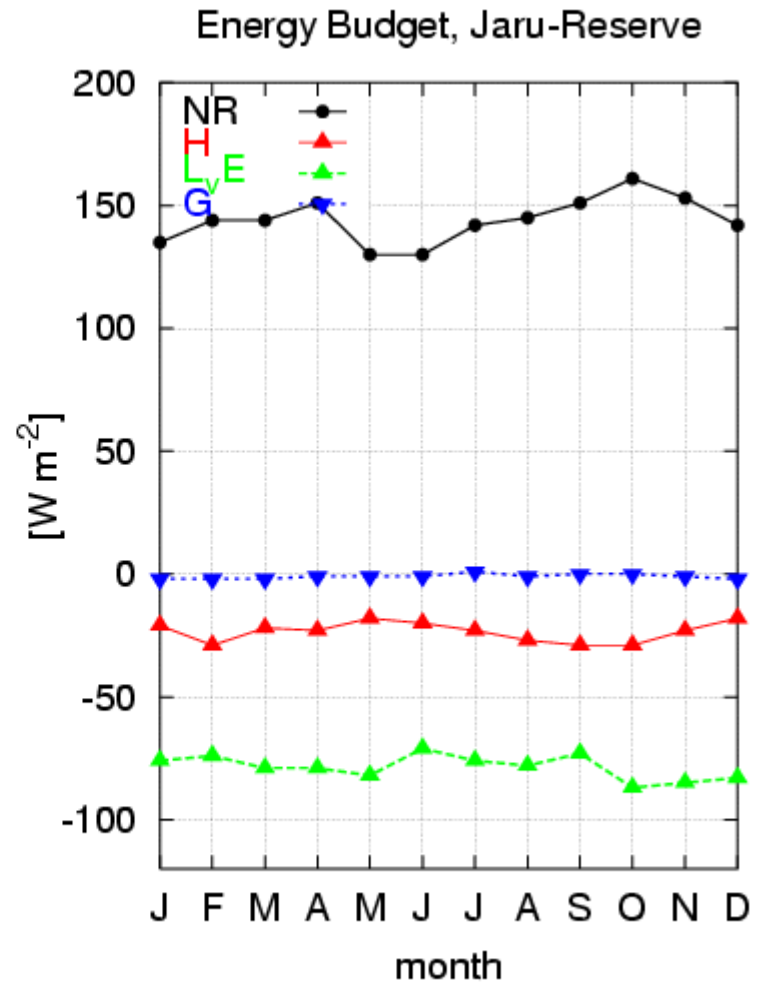
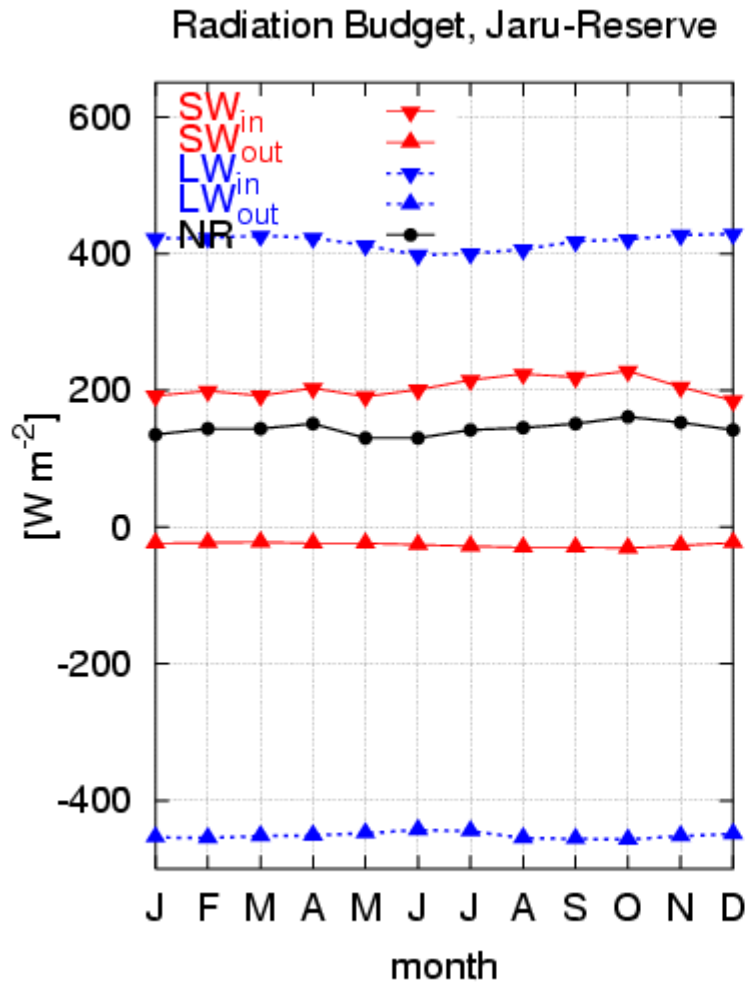
Fig. 10.3b Annual mean distribution of latent heat fluxes, based on data of the re-analysis project ERA-40. This data set covers the period 1991-1995.

A temporal look at the surface energy balance



Grassland site in northeastern Switzerland (8.52°E, 47.43°S)

A temporal look at the surface energy balance (2)

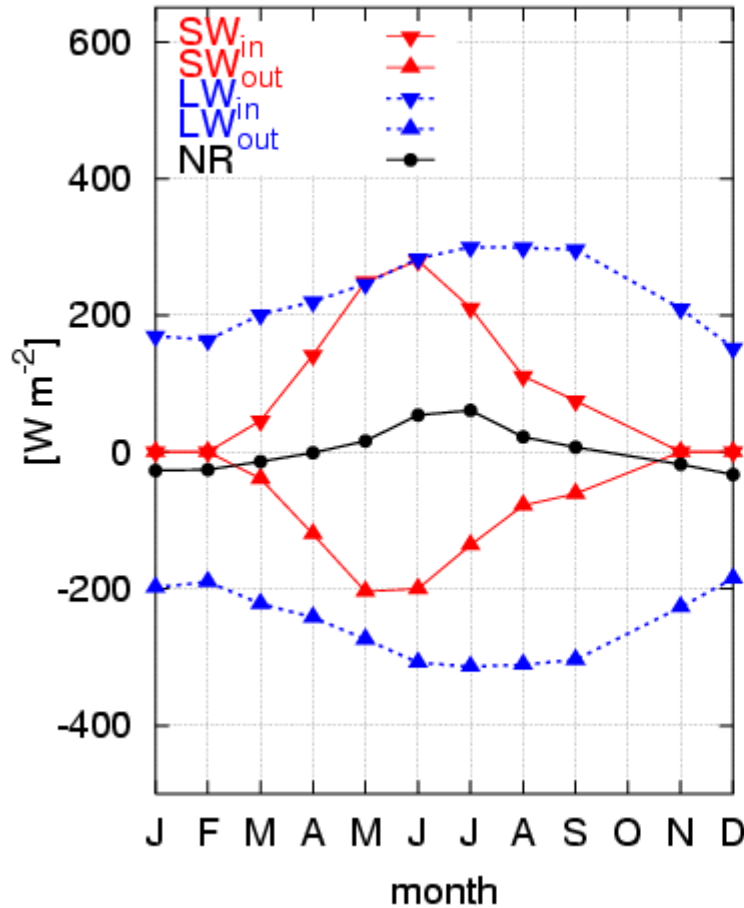


Tropical rain forest in Brazil (State of Rondonia, 61.93°W, 10.08°S)

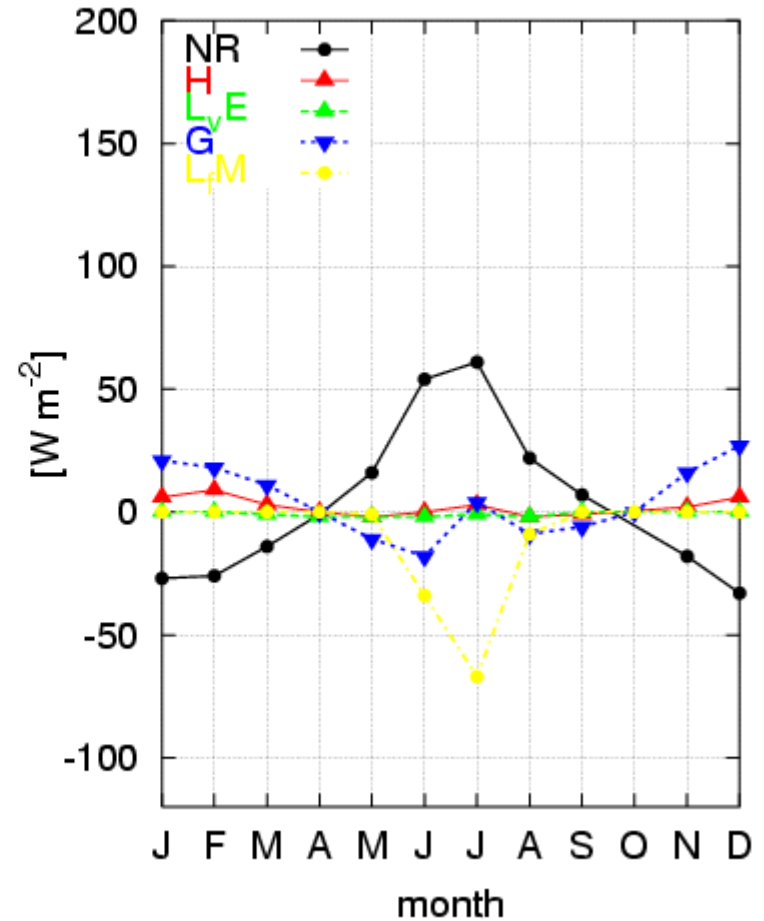
A temporal look at the surface energy balance (3)



Radiation Budget, SHEBA



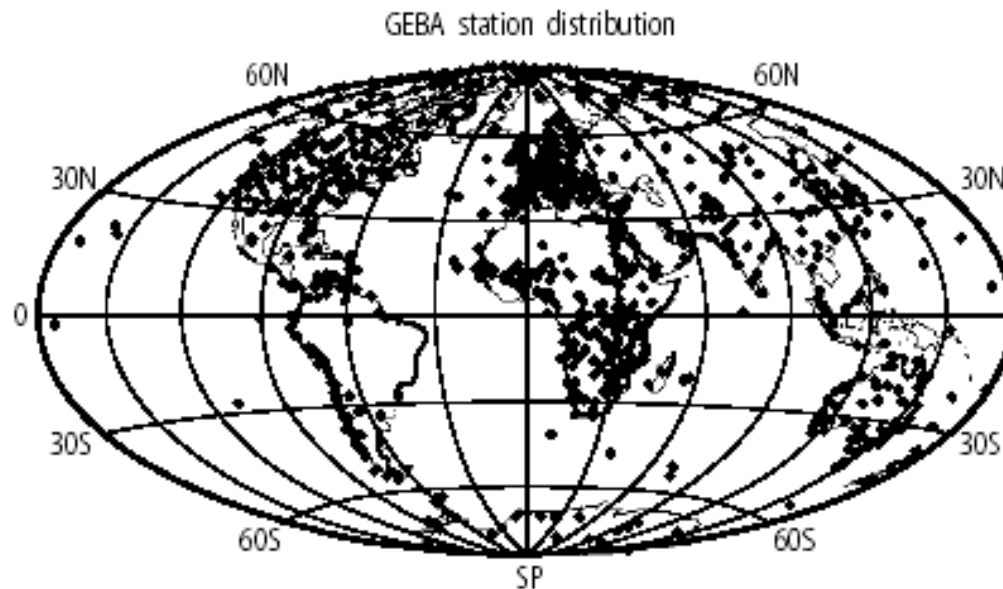
Energy Budget, SHEBA



Arctic sea ice (drifting station, $\sim 160^\circ W$, $75^\circ S$)

An archive of surface energy balance data

Since 1985 data of monthly mean energy fluxes at earth's surface has been collected at ETH by Prof. Ohmura and coworkers, checked for quality and made available for research through GEBA, the Global Energy Balance Archive. GEBA is a project A7 of the World Climate Programme – Water (WMO/ICSU). A description is provided in Gilgen and Ohmura (1999)*

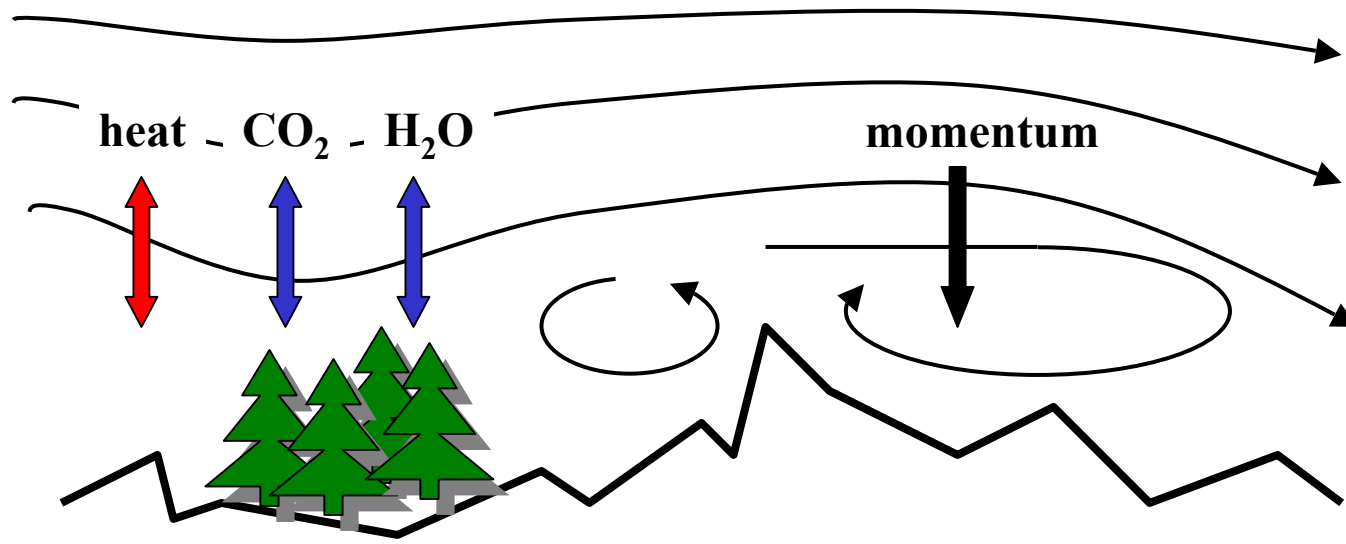


*Gilgen, H. and A. Ohmura, 1999, The Global Energy Balance Archive, Bull. Am. Meteor. Soc., 80(5), 831-850.

Surface processes

The energy exchange is only but one of the possible links between the hydrosphere/biosphere/cryosphere/pedosphere and the atmosphere. Other interactions include:

- the exchange of water;
- the exchange of trace constituents (CO_2 , CH_4 , N_2O , ...);
- the exchange of momentum (friction!)





The atmospheric boundary layer

If we actually look closer at these interactions, we see that they involve not only the very surface but also the atmospheric layer close to the surface. This is the region called the atmospheric or planetary boundary layer (ABL or PBL for short)*.

*For those interested in boundary layer climates, the following books can be recommended:

Brutsaert, W., 1982, *Evaporation into the Atmosphere*, D. Reidel Publishing, Dordrecht, 299 pp.

Budyko, M.I., 1974, *Climate and Life. International Geophysical Series, Vol. 18*. Academic Press, New York, 508 pp.

Garratt, J.R., 1992, *The Atmospheric Boundary Layer*. Cambridge University Press, Cambridge, 316 pp.

Monteith, J.L. and M.H. Unsworth, 1990, *Principles of Environmental Physics*, Second Edition, Edward Arnold, London, 291 pp.

Oke, T.R., 1987: *Boundary Layer Climates*. Second Edition. Routledge, London, 435 pp.

Stull, R.B, 1988, *An Introduction to Boundary Layer Meteorology*, Kluwer, Dordrecht, 666 pp.

The atmospheric boundary layer (2)

The ABL can be defined as the layer of the atmosphere directly affected by the properties of the surface. It can be subdivided as follows (Brutsaert, 1982):

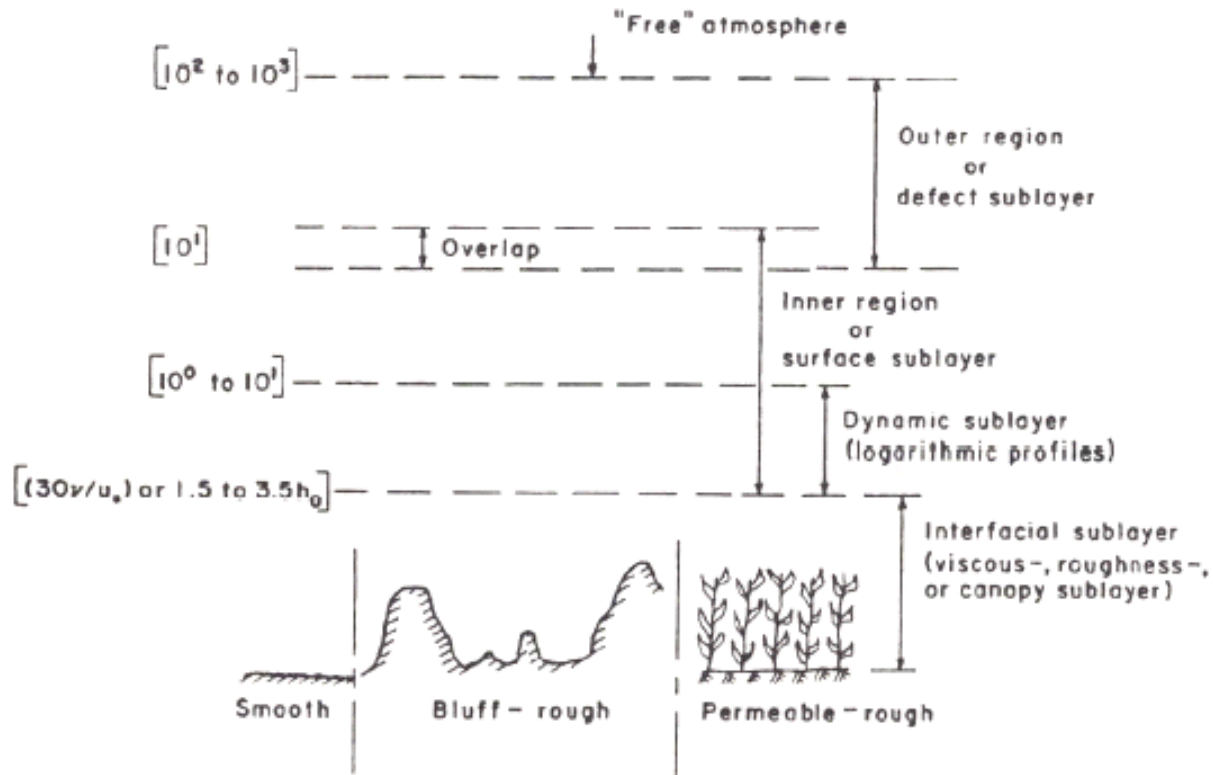


Fig. 3.1. Definition sketch showing orders of magnitude of the heights of the sublayers of the atmospheric boundary layer (ABL); h_0 is a typical height of the roughness obstacles; the (distorted) vertical scale is in meters.

The atmospheric boundary layer (3)

The atmospheric boundary layer continuously evolves in time (Stull, 1988):

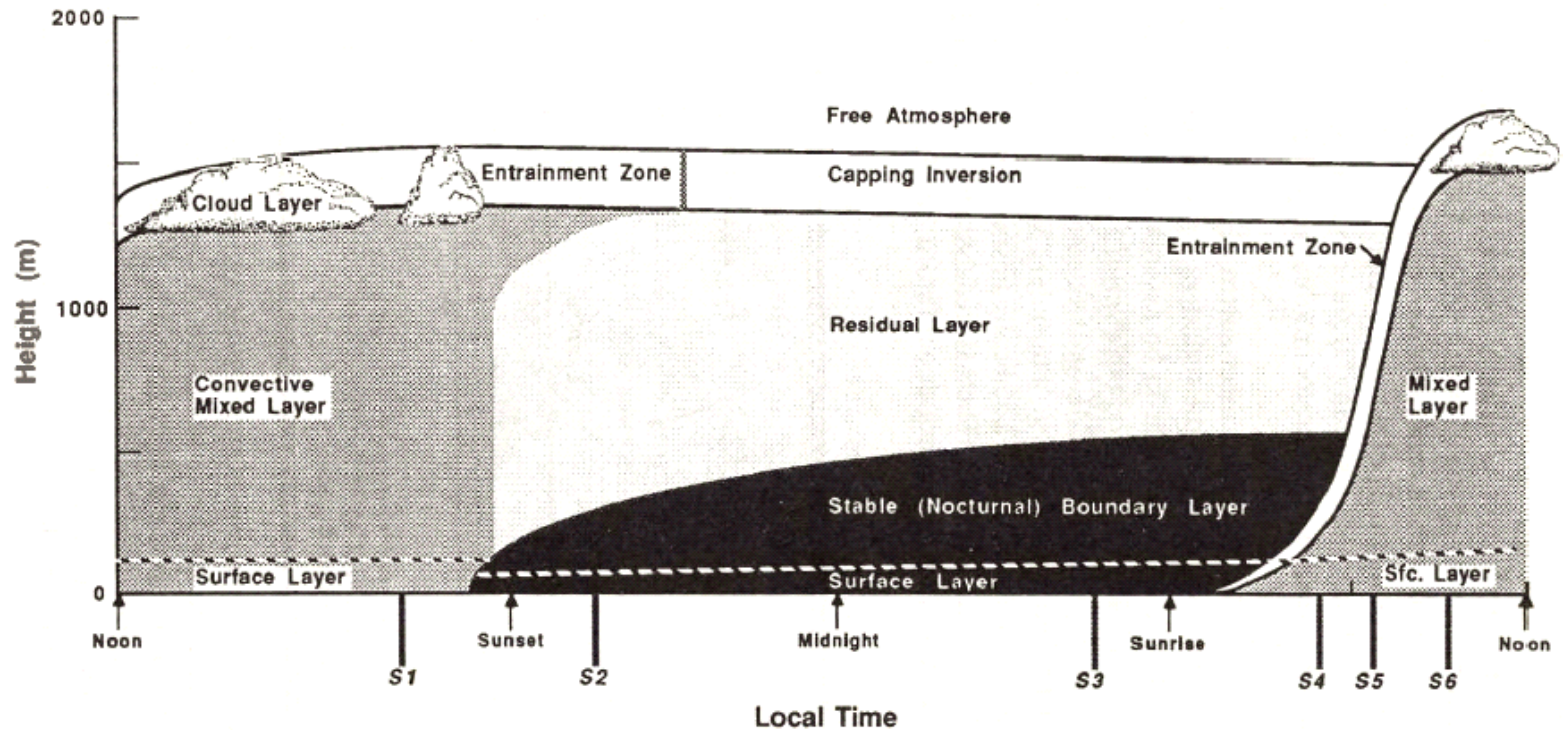
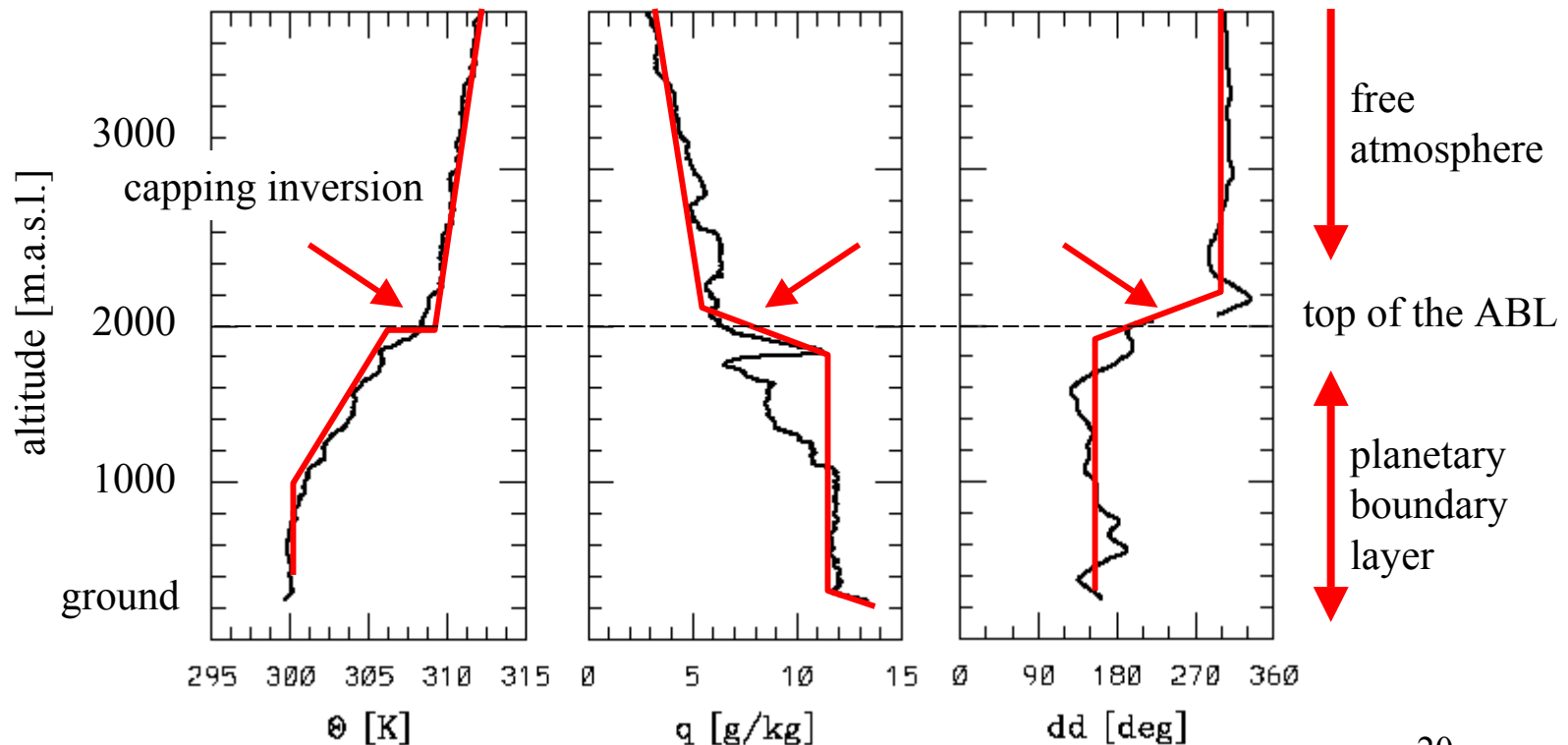


Fig. 1.7 The boundary layer in high pressure regions over land consists of three major parts: a very turbulent mixed layer; a less-turbulent residual layer containing former mixed-layer air; and a nocturnal stable boundary layer of sporadic turbulence. The mixed layer can be subdivided into a cloud layer and a subcloud layer. Time markers indicated by S1-S6 will be used in Fig. 1.12.

The atmospheric boundary layer (4)

The top of the ABL is usually detectable in soundings of the lower atmosphere. The following figures show examples of profiles of the potential temperature, specific humidity and wind direction measured in the upper Ticino on August 25, 1999, 12:00 UTC. They refer to a convective situation. Idealized profiles are superimposed in red.



The atmospheric boundary layer (5)

Another example for the evolution of the ABL is given here (Brutsaert, 1982)

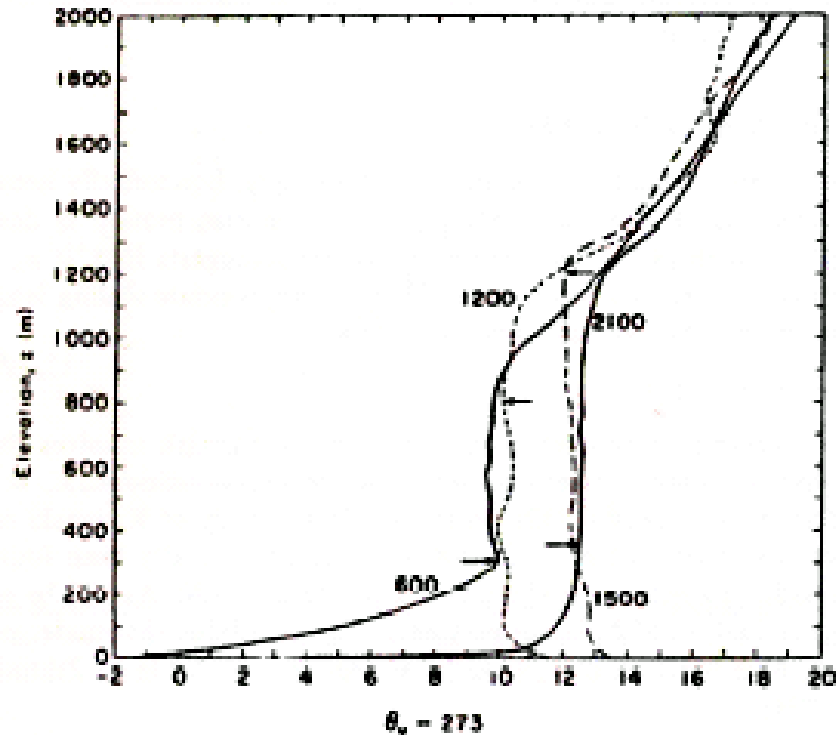


Fig. 4.7. Example of profiles of the virtual potential temperature in and above the atmospheric boundary layer. The estimated values of the height δ , of the boundary layer are indicated by arrows; the numerical values on the profiles indicate times of day. The observations were made by Clarke *et al.* (1971) on July 16, 1967 (Day 33) at Hay, N.S.W., Australia.



Turbulence

One of the essential features of the flow in the ABL is that it is turbulent.

Turbulence can be characterized as follows:

- turbulence is a random (stochastic), 3-dimensional, rotational motion;
- turbulence is non-linear;
- turbulence can only be treated statistically;
- turbulence is diffusive. It efficiently transports momentum, heat, water vapor and other constituents (e.g. CO₂);
- turbulence is dissipative. Molecular viscosity is responsible for the decay of kinetic energy into heat (increase in internal energy at the expense of mechanical energy). To exist turbulence must continuously feed on the 'mean' flow.

The Reynolds number

A distinction between laminar and turbulent flows is possible on the basis of the Reynolds number Re (Batchelor, 1967). For $Re > 2000$, small perturbations of the flow rapidly grow eventually leading to turbulence.

The Reynolds number is defined as the ratio of the inertia and viscous term in the equation of motion. Assuming stationarity:

$$u_k \frac{\partial u_i}{\partial x_k} = -\rho^{-1} \frac{\partial p}{\partial x_i} + \nu \frac{\partial^2 u_i}{\partial x_k \partial x_k}$$

where $\nu \sim 10^{-5} \text{ m}^2 \text{ s}^{-1}$ is the kinematic viscosity. In orders of magnitude, given velocity and length scales U and L :

$$\frac{U^2}{L} \sim -\rho^{-1} \frac{P}{L} + \nu \frac{U}{L^2}$$

whereby, upon building the ratio of the first and last term, one obtains:

$$Re \equiv \frac{U^2 / L}{\nu U / L^2} = \frac{UL}{\nu}$$

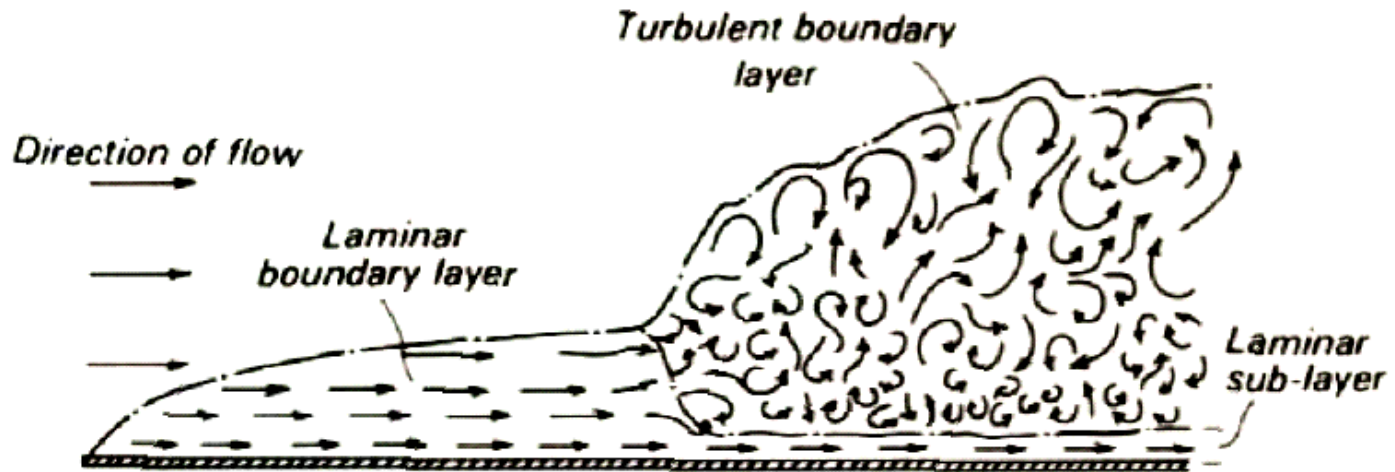
*Batchelor, G.K., 1967, An Introduction to Fluid Dynamics, Cambridge University Press, 610 pp.

ABL flows

In the atmospheric boundary layer $U \sim 1$ to 10 m s^{-1} (a typical wind speed) and $L \sim 1$ to 1000 m (the height above ground). Hence typical values for the Reynolds number are:

$$\text{Re} = \frac{UL}{\nu} \sim \frac{1 \cdot 1}{10^{-5}} \text{ to } \frac{10 \cdot 1000}{10^{-5}} = 10^5 \text{ to } 10^7 \gg 2000$$

It follows that with the exception of a very thin layer close to the surface, ABL flows are always turbulent.



Oke (1987)

Turbulent transfer

In looking at turbulence it is convenient to treat it as a perturbation (u_i' , θ' , q' for the wind components, potential temperature and specific humidity, respectively) of a 'mean' flow (U_i , Θ , Q). That is to say we introduce the so-called Reynolds decomposition:

$$u_i = U_i + u_i', \quad i = 1, 2, 3$$

$$\theta = \Theta + \theta'$$

$$q = Q + q'$$

Turbulent transfer arises from the correlation between the fluctuating components of the flow. With respect to the transfer of momentum, τ , sensible heat, H , and latent heat, $L_v E$, and using the notation $(u, v, w) \equiv (u_1, u_2, u_3)$ for the three components of the wind vector, we have:

$$\tau \equiv -\rho \overline{w'u'}$$

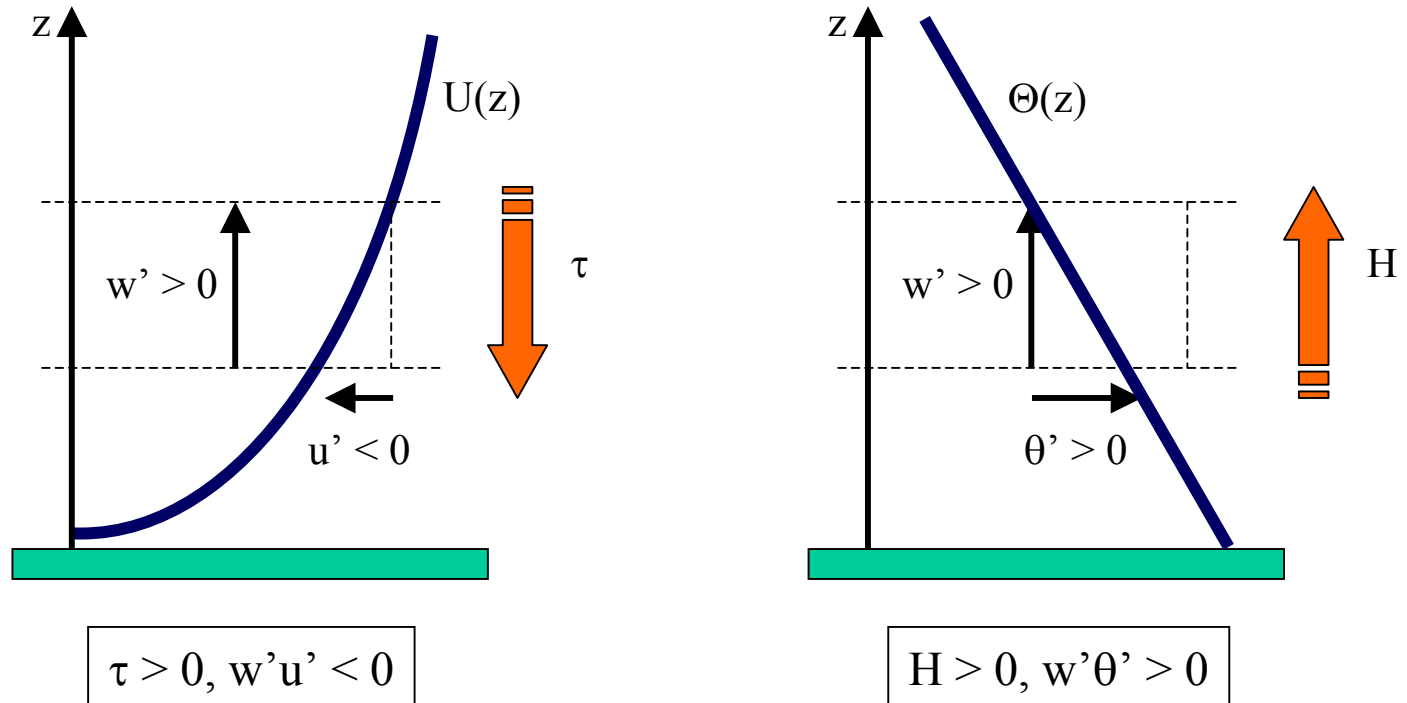
$$H \equiv \rho C_p \overline{w'\theta'}$$

$$L_v E \equiv \rho L_v \overline{w'q'}$$

In boundary layer studies, the shear stress τ is by definition positive when there is an associated transport of momentum to the surface, but H and $L_v E$ are positive when directed away from the surface.

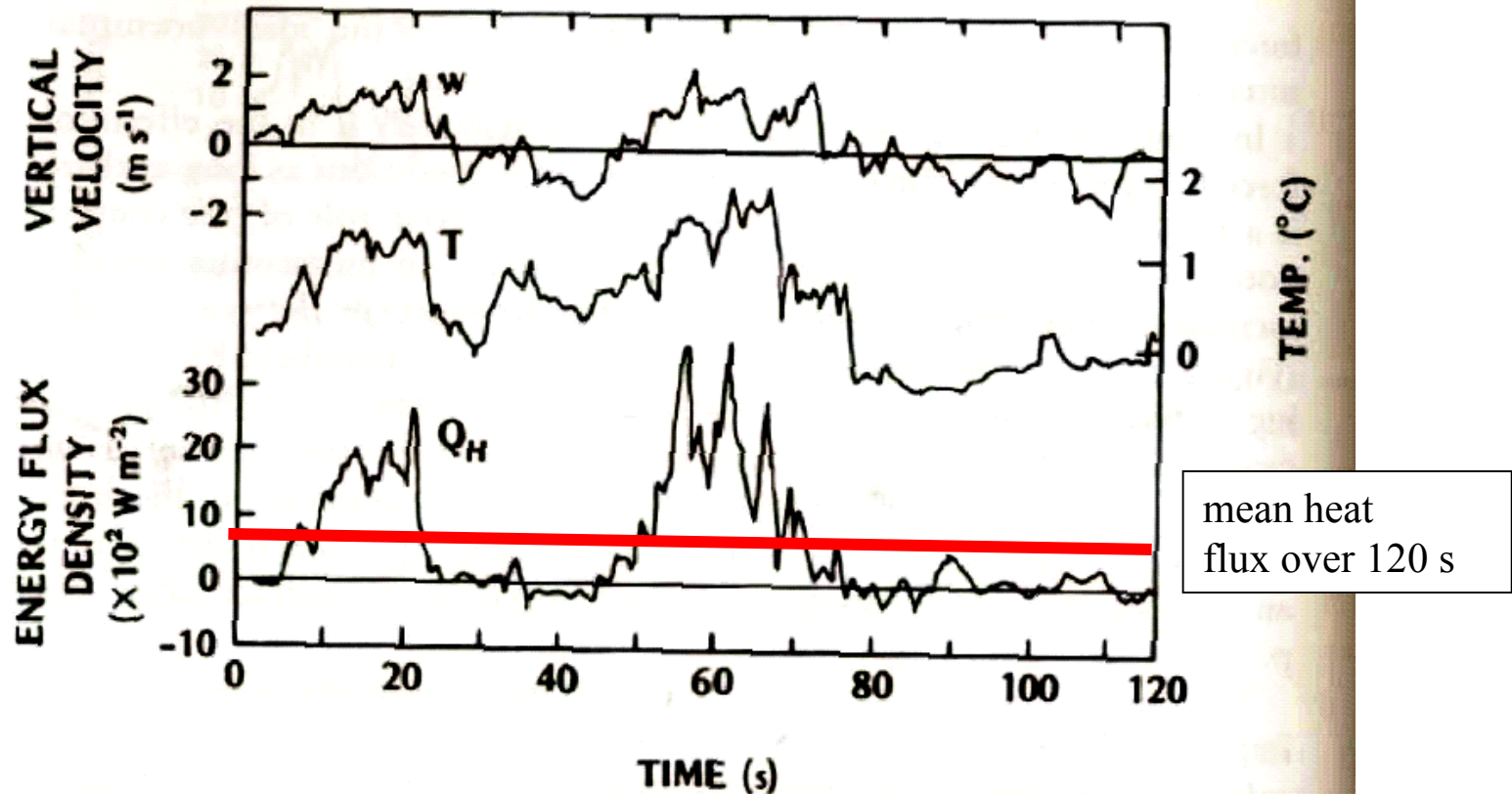
Correlation of fluctuating components

How do we explain the correlation? Consider the following ‘mean’ profiles for the longitudinal wind component $U(z)$ and the potential temperature $\Theta(z)$, the associated shear stress $\tau > 0$ and heat transfer $H > 0$, and the perturbations u' and θ' induced by a vertical displacement $w' > 0$. We have:



Correlation in time series

A succession of correlated perturbations in a time series eventually lead to a statistical correlation over some finite interval of time:



Turbulent fluxes and mean gradients

Fluctuating components and their correlation can be directly measured. However, this type of data is not always available. For this reason, ways for relating the turbulent fluxes to the vertical variations of the mean fields are sought.

There are two basic approaches. In the first, turbulent fluxes are considered in the same way as molecular fluxes. Then:

$$\tau \equiv -\rho \overline{w'u'} = \rho K_M \frac{\partial U}{\partial z}$$

$$H \equiv \rho C_p \overline{w'\theta'} = -\rho C_p K_H \frac{\partial \Theta}{\partial z}$$

$$L_v E \equiv \rho L_v \overline{w'q'} = -\rho L_v K_E \frac{\partial Q}{\partial z}$$

where K_M is the eddy (turbulent) viscosity and K_H and K_E are the eddy diffusivities. All K 's (the 'Austauschkoeffizienten') are in units of $[m^2 s^{-1}]$.

Turbulent fluxes and mean quantities

The second approach makes use of the description of an electrical current I in terms of an electric potential V and a resistance R :

$$I = \frac{V}{R}$$

If this concept is applied to the turbulent transfer, we obtain:

$$\tau \equiv -\rho \overline{w'u'} = \rho \frac{U - U_0}{r_{aM}} = \rho \frac{U}{r_{aM}}$$

$$H \equiv \rho C_p \overline{w'\theta'} = -\rho C_p \frac{\Theta - \Theta_0}{r_{aH}}$$

$$L_v E \equiv \rho L_v \overline{w'q'} = -\rho L_v \frac{Q - Q_0}{r_{aE}}$$

where subscript 0 denotes surface values, and where r_{aM} , r_{aH} and r_{aE} are aerodynamic resistances in units of $[m^{-1} s]$.

A problem with this approach is the fact that the definition of 'surface' values is not always simple.

A general transfer scheme

The description of a 'transfer' in terms of a potential and a resistance can be extended to all scales involved in the interactions between the surface and the atmosphere. Resistances can be put in series or parallel, depending on the format of the transfer. For instance, for the flow of water from the soil, through vegetation, to the atmosphere we can apply the following scheme:

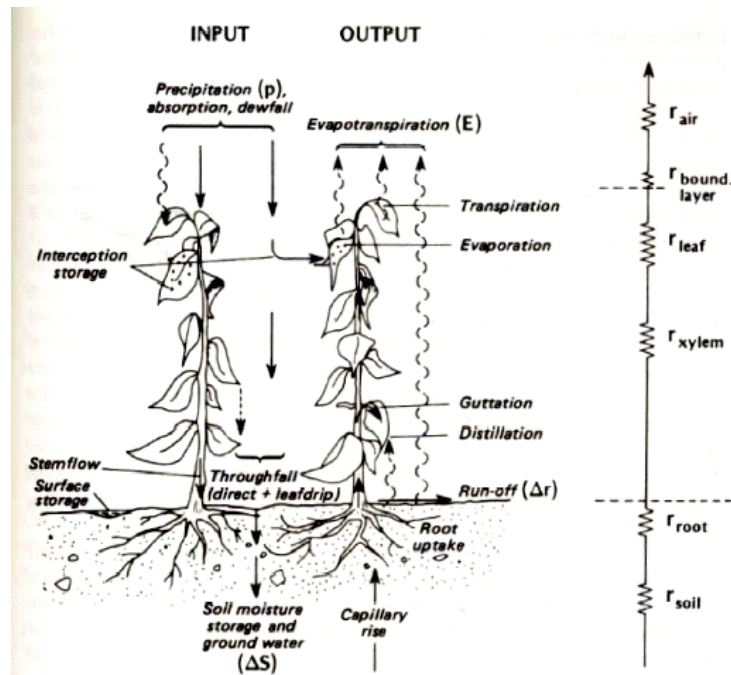


Figure 4.9 The water balance and internal flows of water in a soil-plant-atmosphere system. At the right is an electrical analogue of the flow of water from the soil moisture store to the atmospheric sink via the plant system.

Oke (1987)

Transfer of heat and moisture

Experimental evidence indicates that aerodynamic transfer of heat and moisture through turbulence takes place in complete analogy. In general we assume that to first order $K_M \approx K_H \approx K_E$ and $r_{aM} \approx r_{aH} \approx r_{aE}$.

This allows the Bowen ratio, $Bo \equiv H/L_v E$, to be expressed as:

$$Bo \equiv \frac{\rho C_p \overline{w'\theta'}}{\rho L_v \overline{w'q'}} \approx \frac{C_p \partial\Theta / \partial z}{L_v \partial Q / \partial z} = \frac{C_p \Delta\Theta}{L_v \Delta Q} \approx \frac{C_p (\Theta - \Theta_0)}{L_v (Q - Q_0)}$$

Turbulent transfer and the stability of the atmosphere

Depending on the vertical variation of the potential temperature, the atmosphere can be statically stable, neutral or unstable with respect to adiabatic displacements. We have:

$$\frac{\partial\Theta}{\partial z} > 0 \Rightarrow \text{stable stratification}$$

$$\frac{\partial\Theta}{\partial z} = 0 \Rightarrow \text{neutral stratification}$$

$$\frac{\partial\Theta}{\partial z} < 0 \Rightarrow \text{unstable stratification}$$

Under stable conditions, vertical displacements are limited by buoyancy because denser/lighter fluid finds itself in a lighter/denser environment. This means that also the vertical motion induced by turbulence is reduced or enhanced depending on the sign of $\partial\Theta/\partial z$.

To account for the effects of buoyancy on vertical displacements one introduces a stability correction either in the eddy diffusivities or the aerodynamic resistances.

The Richardson number

On the other hand, turbulence is favored by high wind speeds, which means enhanced friction and mechanical production of instabilities by the wind shear, $\partial U/\partial z$. Therefore, the stability correction applied to the eddy diffusivities or resistances has to be further modified to account for the magnitude of the shear.

There are complementary ways to do so. A widely used possibility is to introduce the so-called Richardson number Ri , which is defined as:

$$Ri \equiv \frac{g}{\Theta_{\text{ref}}} \frac{\partial \Theta / \partial z}{(\partial U / \partial z)^2}$$

The numerator being always positive, the combined effects of stability and shear on turbulent transfer can be expressed as:

- $Ri > 0 \Rightarrow$ stable conditions
- $Ri = 0 \Rightarrow$ neutral conditions
- $Ri < 0 \Rightarrow$ unstable conditions

The logarithmic wind profile

Two important parameters needed to describe the aerodynamic state of the flow are the friction velocity u_* and the roughness length z_0 . The friction velocity is defined as:

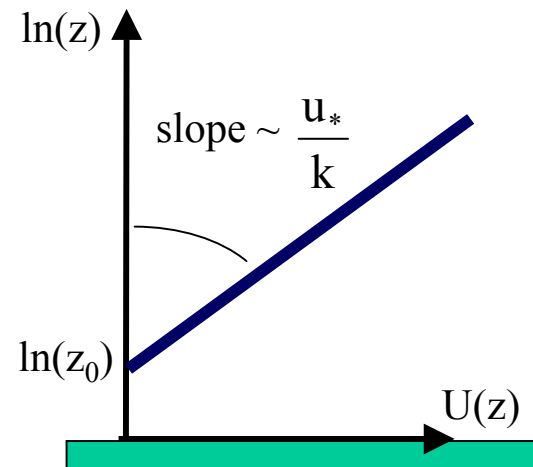
$$u_* \equiv \sqrt{\frac{\tau}{\rho}}$$

whereas the roughness length is the height at which $U = 0$. It is related to the geometric properties of the surface.

Together they characterize the shape of the so-called logarithmic wind profile, the vertical variation of wind speed under neutral conditions:

$$U(z) = \frac{u_*}{k} \ln\left(\frac{z}{z_0}\right)$$

where $k = 0.4$ is the von-Kármán constant.



Explicit expression for K_M

Given the wind profile and the definition of the friction velocity, we can find explicit expressions for the eddy diffusivities and the aerodynamic resistances. We also need the first derivative of the wind profile, which in neutral conditions reads:

$$U(z) = \frac{u_*}{k} \ln\left(\frac{z}{z_0}\right) \Rightarrow \frac{\partial U}{\partial z} = \frac{u_*}{k z}$$

Then:

$$\tau = -\rho K_M \frac{\partial U}{\partial z} = -\rho K_M \frac{u_*}{k z} = \rho u_*^2$$

and by equating the last two terms:

$$K_M = k z u_*$$

To account for stability we usually write:

$$K_M = \frac{k z u_*}{\Phi(Ri)}$$

where Φ is a known function of the Richardson number.

Explicit expression for r_{aM}

To arrive at explicit expressions for the resistances we introduce the wind profile directly into the definition of the shear stress:

$$\tau = \rho u_*^2 = \rho \frac{k^2 U^2}{\{\ln(z/z_0)\}^2} = \rho \frac{U}{r_{aM}}$$

showing that either:

$$r_{aM} = \frac{U}{u_*^2}$$

or, in neutral conditions:

$$r_{aM} = \frac{\{\ln(z/z_0)\}^2}{k^2 U}$$

To account for stability we usually write:

$$r_{aM} = \frac{\{\ln(z/z_0) - \Psi(Ri)\}^2}{k^2 U}$$

where Ψ is another known function of the Richardson number.

Aerodynamic properties of natural surfaces

Table 2.2 Aerodynamic properties of natural surfaces

Surface	Remarks	z_0 Roughness length (m)	d Zero plane displacement* (m)
Water†	Still – open sea	$0.1 - 10.0 \times 10^{-5}$	–
Ice	Smooth	0.1×10^{-4}	–
Snow		$0.5 - 10.0 \times 10^{-4}$	–
Sand, desert		0.0003	–
Soils		0.001–0.01	–
Grass†	0.02–0.1 m	0.003–0.01	≈ 0.07
	0.25–1.0 m	0.04–0.10	≈ 0.66
Agricultural crops†		0.04–0.20	≈ 3.0
Orchards†		0.5–1.0	≈ 4.0
Forests†	Deciduous	1.0–6.0	≈ 20.0
	Coniferous	1.0–6.0	≈ 30.0

* Only approximate, calculated as $d = \frac{2}{3}h$ (see p. 116)

† z_0 depends on wind speed (see p.139)

Sources: Sutton (1953), Szeicz *et al.* (1969), Kraus (1972).

Heat transfer in soil

The rate at which heat flows through a soil at a depth z below the surface is directly proportional to the temperature gradient:

$$G = -\lambda \frac{\partial T}{\partial z}$$

where λ is the thermal conductivity [$\text{W m}^{-1} \text{K}^{-1}$].

Changes of G with depth lead to changes in time of the heat content of the soil:

$$\frac{\partial T}{\partial t} = -\frac{1}{C} \frac{\partial G}{\partial z}$$

where C is the heat capacity [$\text{J m}^{-3} \text{K}^{-1}$].

Combining the two equations and assuming that the thermal conductivity does not vary with depth, we arrive at a second-order partial differential equation for the soil temperature:

$$\frac{\partial T}{\partial t} = -\frac{1}{C} \frac{\partial}{\partial z} \left(-\lambda \frac{\partial T}{\partial z} \right) = \frac{\lambda}{C} \frac{\partial^2 T}{\partial z^2} \equiv \kappa \frac{\partial^2 T}{\partial z^2}$$

where $\kappa = \lambda/C$ is the thermal diffusivity [$\text{m}^2 \text{s}^{-1}$].

Heat transfer in soil (2)

To obtain a solution we must specify an initial as well as a boundary condition. We assume that at the surface ($z = 0$) temperature can be described as:

$$T(0, t) = \langle T \rangle + \Delta T_0 \sin(\omega t)$$

where

$\langle T \rangle$ = mean (daily or annual) soil temperature
(assumed to be the same at all depths)

ΔT_0 = $0.5 \cdot (T_{\max} - T_{\min})$, the amplitude of the surface wave

ω = $2\pi/P$ the angular frequency

P = period of the oscillation
(24 hours or 12 months or 365 days).

With this boundary condition:

$$T(z, t) = \langle T \rangle + \Delta T_0 e^{-z\sqrt{\omega/2\kappa}} \sin(\omega t - z\sqrt{\omega/2\kappa})$$

Note that $\sqrt{2\kappa/\omega}$ has dimensions of depth or units of [m]. Therefore writing $z \sqrt{\omega/2\kappa}$ is equivalent to z / z_e , and this shows that $z_e = \sqrt{\omega/2\kappa}$ is the depth at which the amplitude of the temperature fluctuation has decayed to e^{-1} of its surface value. 39

Heat transfer in soil (3)

At any given depth z , the amplitude of the daily or annual cycle is:

$$\delta = \Delta T_0 e^{-z\sqrt{\omega/2\kappa}}$$

and the time of maximum soil temperature is found by setting:

$$\sin(\omega t - z\sqrt{\omega/2\kappa}) = 1$$

or:

$$t_{\max} = \frac{1}{\omega} \left(\frac{\pi}{2} + z\sqrt{\omega/2\kappa} \right)$$

Using the solution $T(z,t)$ we can finally calculate $G(z,t)$ as follows :

$$G(z,t) = \Delta T_0 \sqrt{\omega C \lambda} e^{-z\sqrt{\omega/2\kappa}} \sin \left(\omega t - z\sqrt{\omega/2\kappa} + \frac{\pi}{4} \right)$$

Thermal properties of natural materials

Table 2.1 Thermal properties of natural materials

Material	Remarks	ρ Density (kg m^{-3} $\times 10^3$)	c Specific heat ($\text{J kg}^{-1} \text{K}^{-1}$ $\times 10^3$)	C Heat capacity ($\text{J m}^{-3} \text{K}^{-1}$ $\times 10^6$)	k Thermal conductivity ($\text{W m}^{-1} \text{K}^{-1}$)	κ Thermal diffusivity ($\text{m}^2 \text{s}^{-1}$ $\times 10^{-6}$)	μ Thermal admittance ($\text{J m}^{-2} \text{s}^{-1/2} \text{K}^{-1}$)
Sandy soil (40% pore space)	Dry	1.60	0.80	1.28	0.30	0.24	620
	Saturated	2.00	1.48	2.96	2.20	0.74	2550
Clay soil (40% pore space)	Dry	1.60	0.89	1.42	0.25	0.18	600
	Saturated	2.00	1.55	3.10	1.58	0.51	2210
Peat soil (80% pore space)	Dry	0.30	1.92	0.58	0.06	0.10	190
	Saturated	1.10	3.65	4.02	0.50	0.12	1420
Snow	Fresh	0.10	2.09	0.21	0.08	0.10	130
	Old	0.48	2.09	0.84	0.42	0.40	595
Ice	0°C, pure	0.92	2.10	1.93	2.24	1.16	2080
Water*	4°C, still	1.00	4.18	4.18	0.57	0.14	1545
Air*	10°C, still	0.0012	1.01	0.0012	0.025	21.50	5
	Turbulent	0.0012	1.01	0.0012	~125	~ 10×10^6	390

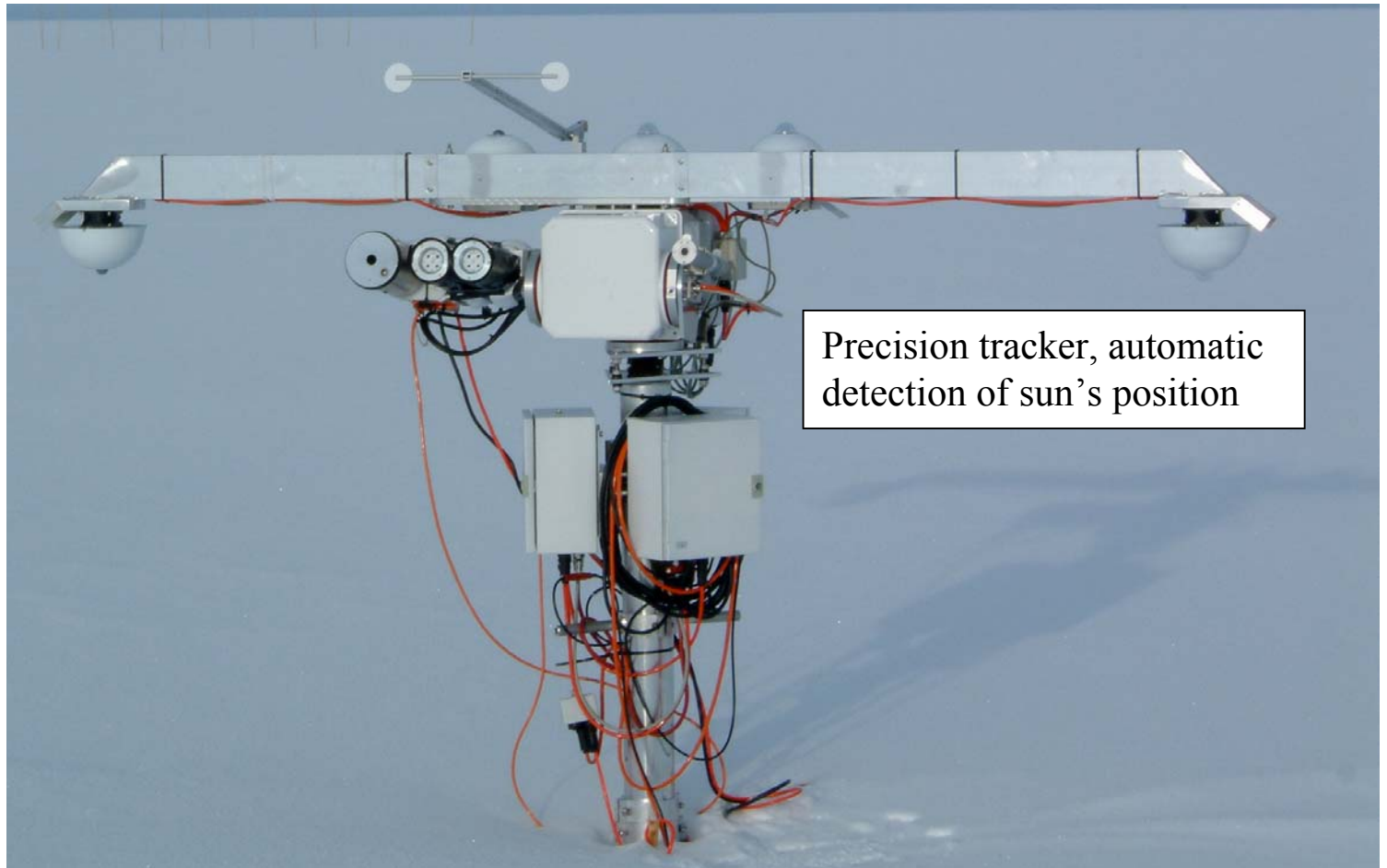
* Properties depend on temperature, see Appendix A3.

Sources: van Wijk and de Vries (1963), List (1966).

Oke (1987)

The thermal properties of soil depend on soil type (fractions), and the content of air, water, ice, organic matter. A good overview can be found in: Sellers, W.D., 1965, *Physical Climatology*, The University of Chicago Press, Chicago, 272 pp.

Observing systems: radiation



IACETH, Greenland (2006)

Observing systems: radiation



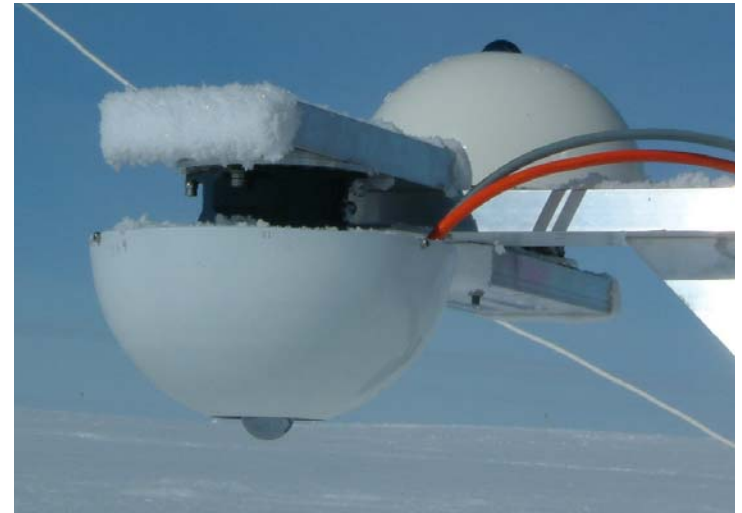
Cavity radiometer (direct solar radiation).
Measures in the wavelength range
335 to 2200 nm (0.33 to 2.2 μm).

IACETH, Greenland (2006)

Pyranometer (solar radiation).
Schott K5 dome, 335-2200 nm.



Precision Infrared Radiometer (PIR)
(longwave radiation). Si-dome + interference
filter. Measures in the wavelength range
 ~ 4 to 50 μm .



Observing systems: mean profiles



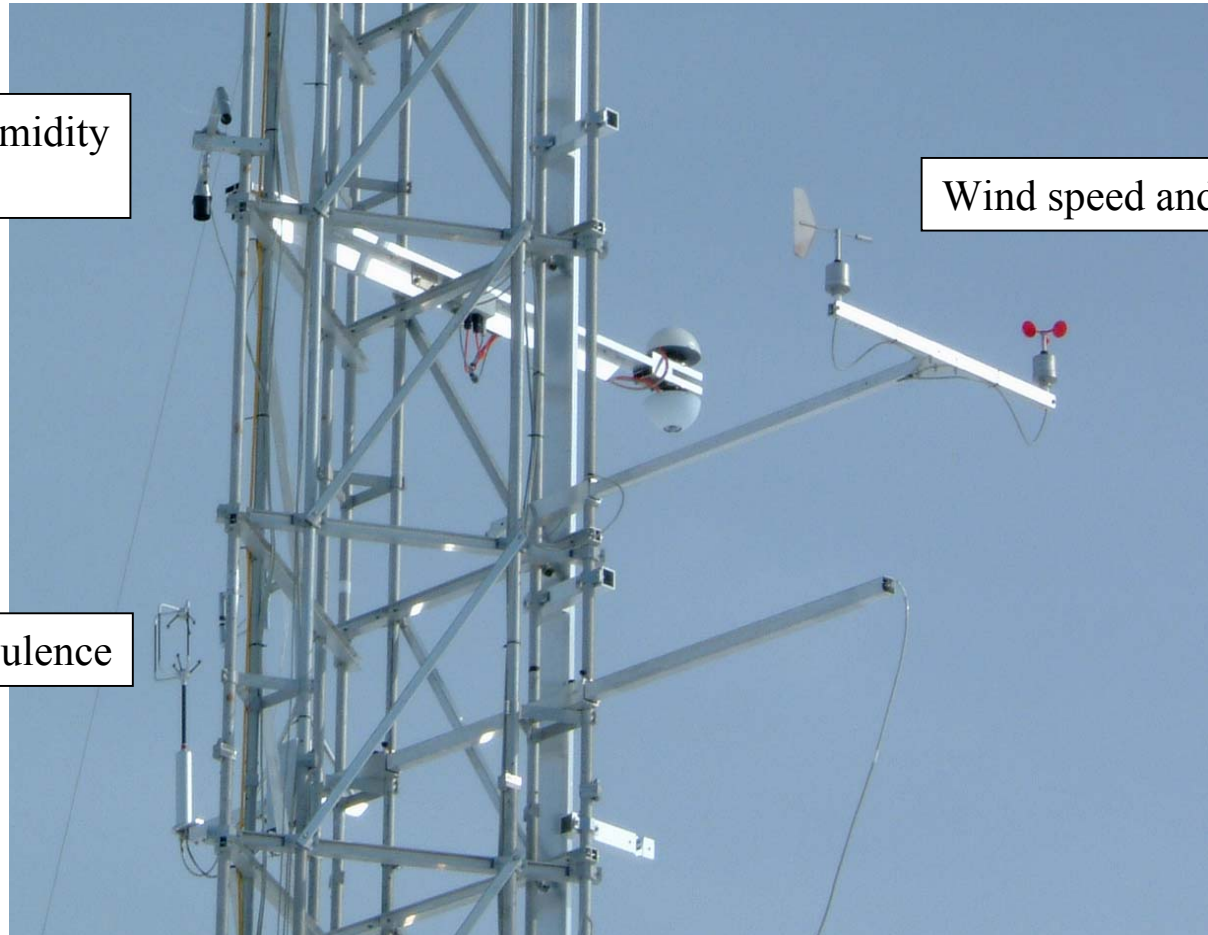
CARBOEUROPE (2006)

Observing systems: mean quantities

Temperature and air humidity
(aspirated instruments)

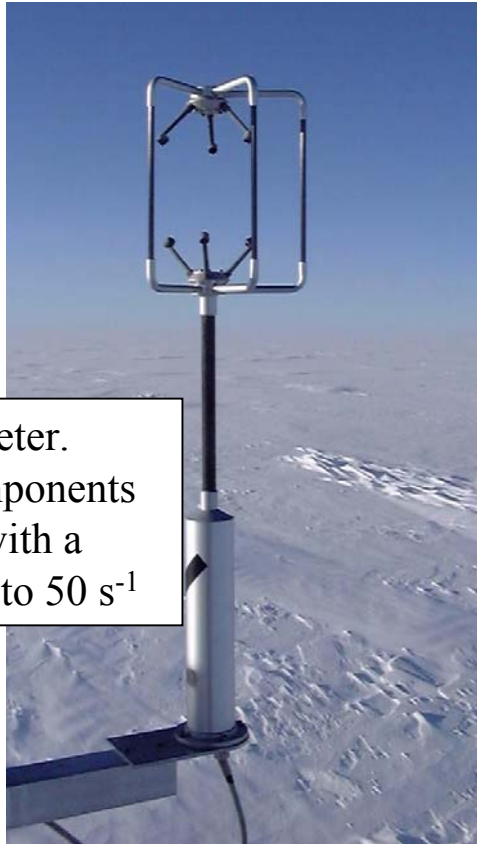
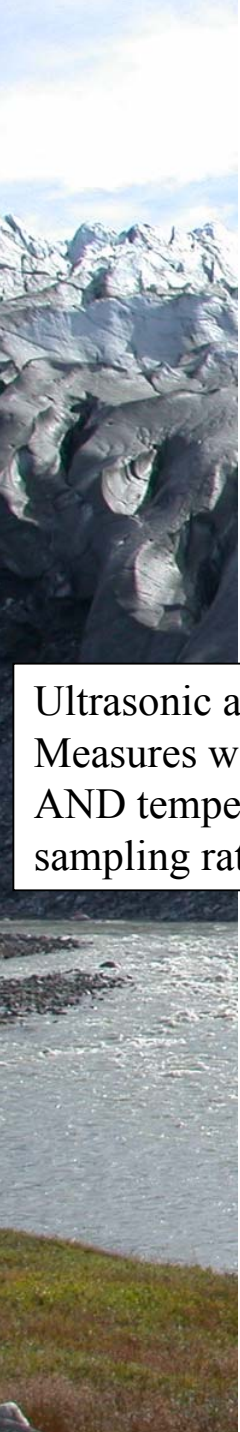
Wind speed and direction

Turbulence



IACETH, Greenland (2006)

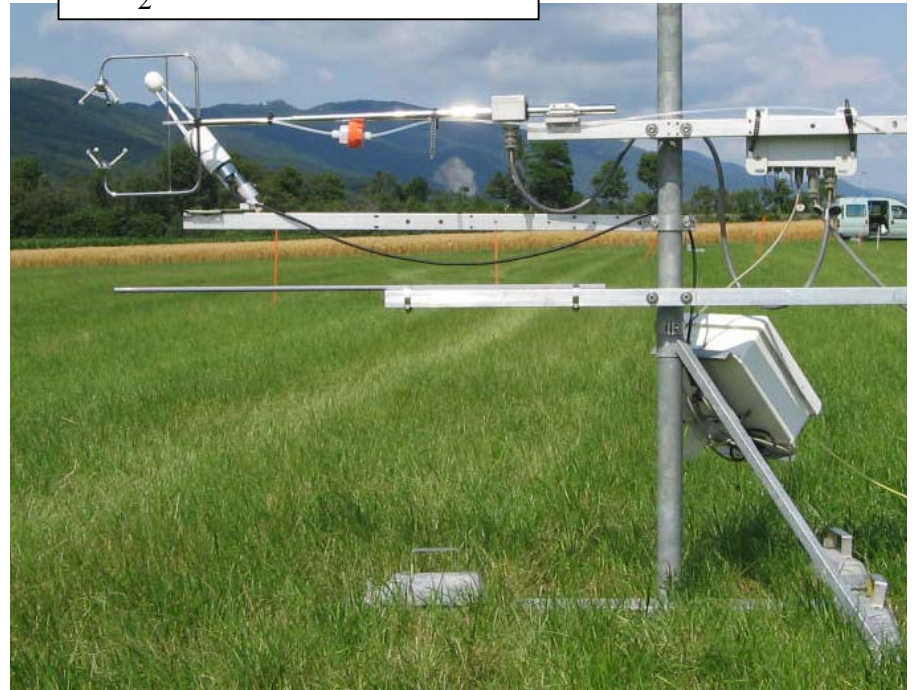
Observing systems: turbulence



Ultrasonic anemometer.
Measures wind components
AND temperature with a
sampling rate of 20 to 50 s⁻¹

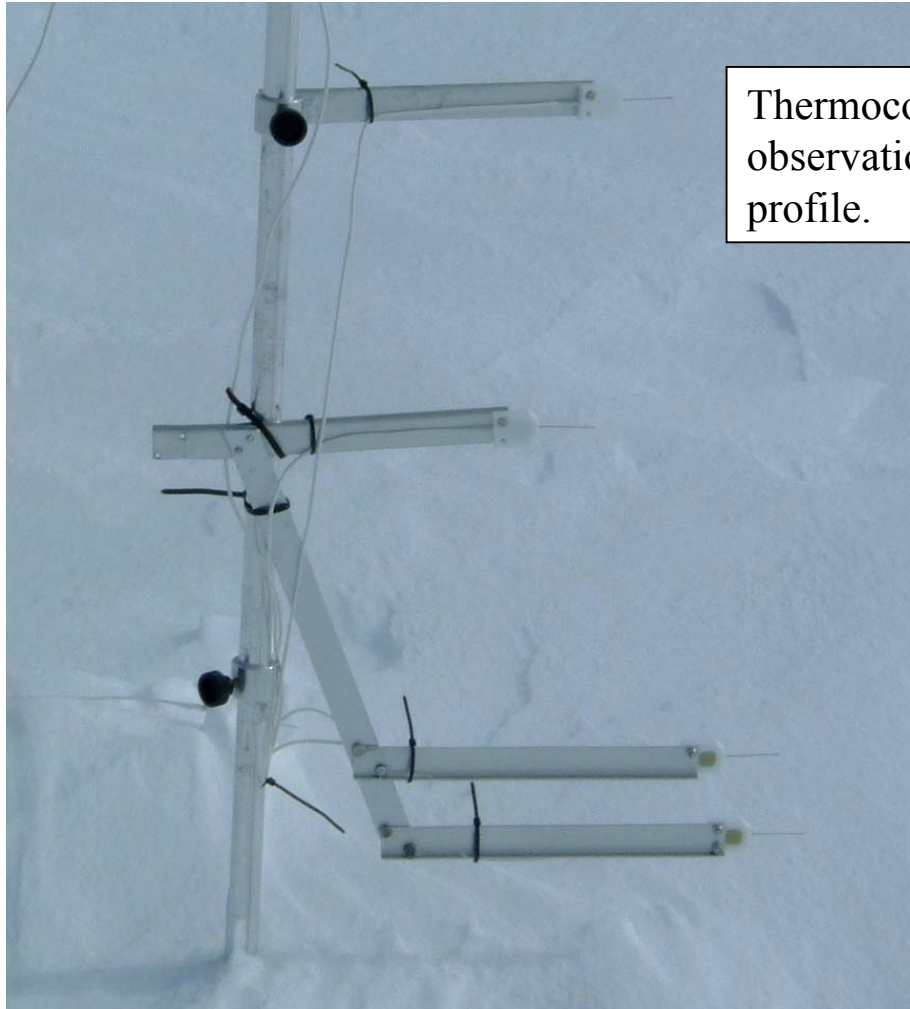
LACETH, Greenland (2006)

Ultrasonic anemometer +
fast-response H₂O and
CO₂ sensors



Agroscope Reckenholz (2006)

Observing systems: temperature profile

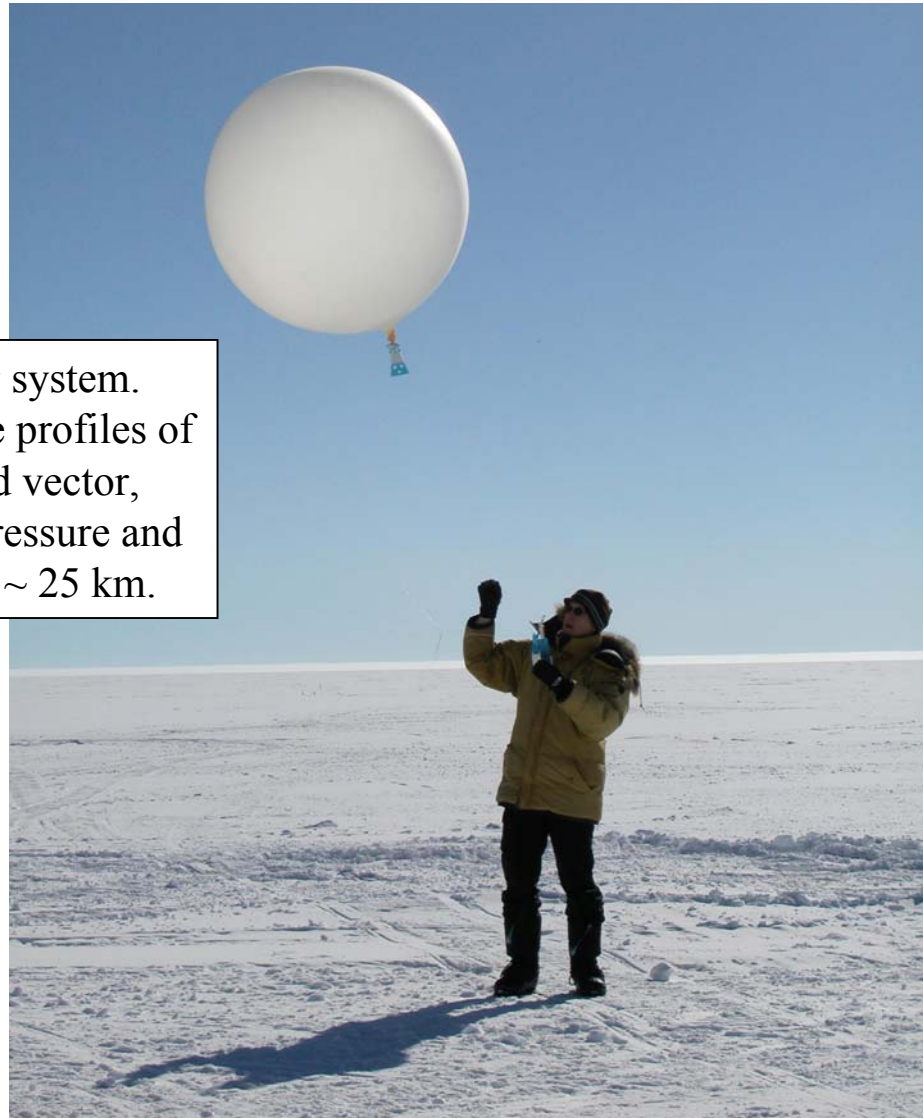


Thermocouples. Use for detailed observations of the temperature profile.

IACETH, Greenland (2006)

Observing systems: boundary layer and free atmosphere

Radiosounding system.
Use to measure profiles of
horizontal wind vector,
temperature, pressure and
humidity up to ~ 25 km.



IACETH, Greenland (2006)